

PCSK7: A Potential Target for Treatment of Non-Alcoholic Fatty Liver Disease (NAFLD)

Sahar Mikaeeli



Department of Medicine
Division of Experimental Medicine
McGill University
Montreal, Canada
February 2021

Laboratory of Biochemical Neuroendocrinology
Clinical Research Institute of Montreal (IRCM)
Montréal, Quebec, Canada

Abstract:

Non-alcoholic fatty liver disease (NAFLD) is a high prevalence disorder that affects more than 25% of American adults and refers to a condition where there is an accumulation of surplus fat in the liver. Up to now, there is no approved drug for therapy for the earlier reversible stages. The export of lipids in very-low-density lipoproteins (VLDL) is an important mechanism involved in lipid disposal in the liver. Deficiencies in different parts of this pathway could result in triglycerides (TG) accumulation and steatosis. There are two important proteins associated with NAFLD that are involved in VLDL secretion and lipidation.

The proprotein convertase 7 (PC7) is the 7th serine protease member (out of 9) of the proprotein convertase family. Very recent investigation in our lab showed that PC7 can act as a chaperone enhancing the folding of ApoB, and the liver of PC7 knockout (KO) mice have ~50% lower ApoB protein levels in both the liver and plasma compared to PC7 wild type (WT) mice. Also, our GWAS studies demonstrated that the gain-of-function (GOF) variant (rs236918) of *PCSK7* is associated with 3.5% elevated plasma TG levels ($p=4.6 \times 10^{-119}$), while the loss-of-function (LOF) variant (rs142953140; R504H), is associated with ~30% reduced TG in human. According to these results, and our own studies showing non-enzymatic functions of PC7 in the regulation of ApoB levels in the endoplasmic reticulum, silencing *PCSK7* could represent a potential therapeutic target for the treatment of NAFLD.

In this project, we designed and evaluated a promising knockdown Antisense Oligonucleotides (ASOs) strategy for silencing *PCSK7* for the eventual treatment of NAFLD.

Our results from this project showed that some selected ASOs can successfully decrease the *PCSK7* mRNA and PC7 protein levels. Indeed, Functional assays were performed aimed to

measure the number and size of TG-rich cytosolic lipid droplets (LD) in hepatic cells. The results showed a highly significant decrease in the number of LDs in both human and mouse hepatocytes transfected with ASOs to *PCSK7* in comparison with those transfected with control scrambled ASOs.

Another important protein associated with NAFLD is the transmembrane 6 superfamily 2 (TM6SF2). The most common TM6SF2 LOF SNP is E167K, which is associated with Alcoholic Fatty Liver Disease (AFLD) and Nonalcoholic Fatty Liver Disease (NAFLD). TM6SF2 promotes the lipidation of VLDL particles by transporting neutral lipids from intermediate low density (ILD) to very low density (VLDL) particles. Recent investigations showed that TM6SF2 and ApoB proteins stabilize each other by forming a complex in the ER. These results suggested that TM6SF2 and *PC7* may interact with each other as both affect the ApoB protein levels and regulate its levels in the liver.

Preliminary results indicated that siRNA silencing of *TM6SF2* results in a significant reduction in *PC7* mRNA and protein levels. However, the absence of *PC7* does not lead to any significant change in the TM6SF2 protein and mRNA levels. Furthermore, co-expression of TM6SF2 WT, TM6SF2 E167K, and TM6SF2 S165E with *PC7*-WT in IHH and HepG2 cells showed a significant decrease of *PC7* levels but not those of its zymogen pro*PC7*, suggesting that TM6SF2 may bind to pro*PC7* and that it may regulate the function of *PC7*.

Résumé:

La stéatose hépatique non alcoolique (SHNA) est une pathologie fréquente qui affecte jusqu'à 25% des adultes Américains et consiste en une accumulation d'excès de gras dans le foie de personnes buvant peu ou pas d'alcool. Jusqu'à présent aucun médicament efficace n'a encore été approuvé pour le traitement de la SHNA. Le contrôle de la diète et l'exercice sont fortement recommandés durant les stades précoces de cette maladie. L'export de lipides sous forme de lipoprotéines de très basse densité (LTBD) est un mécanisme essentiel utilisé dans la disposition des lipides du foie. Des déficiences de différentes composantes de ce mécanisme pourraient mener à une accumulation de triglycérides (TG) et une stéatose hépatique. Dans cette thèse nous avons élaboré des traitements oligonucleotide antisense pour bloquer l'expression de deux protéines impliquées dans la SHNA, soit la PC7 et la TM6SF2, toutes deux impliquées dans la régulation de l'apolipoprotéine B (ApoB), sa lipodation et la sécrétion des LTBD.

La proprotéine convertase 7 (PC7) est une sérine protéase sécrétoire représentant le 7^{ie} membre (sur un total de 9) de la famille des proprotéines convertases. Des résultats récents de notre laboratoire ont démontré que la PC7 pourrait agir comme chaperonne moléculaire qui assisterait le repliement de l'ApoB dans le réticulum endoplasmique (RE), et que les KO de PC7 dans le foie de souris présentent une réduction de ~50% des niveaux hépatiques et plasmatiques de l'ApoB, comparées aux souris du type sauvage. De plus, nos résultats GWAS encore non publiés démontrent que le variant du type gain-de-fonction intronique de la *PCSK7* humaine (rs236918) est associé à une augmentation de 3.5% des niveaux plasmatiques des TG ($p=4.6 \times 10^{-119}$). En corollaire le variant codant (R504H; rs142953140) menant à une perte-de-fonction de la PC7 est associé çà une diminution de ~30% des TGs circulants chez l'humain. Basé sur toutes ces données

la réduction du niveau des RNAm de la *PCSK7* pourrait potentiellement mener vers un nouveau traitement thérapeutique pour contrer le développement de la SHNA. Pour ceci, nous avons conçu et évalué le potentiel d'oligonucléotides antisenses (OAS) contre la *PCSK7* pour le traitement éventuel de la SHNA.

Nos résultats ont démontré que certains des OAS choisis réduisent considérablement les niveaux des ARNm de la *PCSK7* et de la protéine PC7. Des essais fonctionnels ont aussi établi que ces OAS diminuent considérablement les gouttelettes lipidiques (GL; riches en TGs) dans les cellules hépatiques humaines et de souris. La prochaine étape serait d'injecter ces OAS (modifiés avec des chaînes galactosamine pour le ciblage efficace au foie) chez la souris et de vérifier leurs effets *in vivo* sur les TGs et l'ApoB.

Une autre protéine associée à la SHNA est la 'transmembrane 6 superfamily 2' (TM6SF2). En effet un variant commun E167K de la TM6SF2 (perte-de-fonction) est associé au développement de la SHNA. TM6SF2 favorise la lipidation des LTBD en augmentant l'échange de lipides à partir de gouttelettes lipidiques cytosoliques vers les particules naissantes des LTBD. Des données récentes démontrent que TM6SF2 et ApoB forment un complexe stable dans le RE. Comme PC7 et ApoB aussi forment un complexe dans RE, on a émis l'hypothèse que TM6SF2 pourrait influencer les niveaux de PC7 et donc de l'ApoB dans le foie.

Nos résultats préliminaires ont indiqué que l'absence de TM6SF2 réduirait les taux de la PC7 au niveau des ARNm et de la protéine, mais qu'en absence de PC7 les niveaux de TM6SF2 ne sont pas affectés. Finalement, les co-expressions de TM6SF2 WT, TM6SF2 E167K, and TM6SF2 S165E avec PC7-WT dans les cellules IHH and HepG2 démontrent une diminution significative des niveaux de PC7 mature mais pas de son zymogène proPC7, suggérant que la TM6SF2 pourrait lier proPC7 et serait donc un nouveau régulateur de PC7 et de ses fonctions biologiques.

Acknowledgements

Foremost, I would like to express my special appreciation and thanks to my supervisor, Dr. Nabil G. Seidah, as a tremendous mentor. I would like to thank him for his patience, support, invaluable pieces of advice, and endless encouragement through all the way in my master's studies. This work would not have been possible without his support and enthusiasm.

Likewise, I would also like to thank Dr. Annik Prat, Mouna Derbali, Delia Susan-Resiga, Ali Ben Djoudi Ouadda, Rachid Essalmani, as well as current and previous research assistants: Ann Chamberland, Anna Roubtsova, Alexandra Evagelidis, Edwidge Marcinkiewicz for their technical support and invaluable pieces of advice and training me in molecular biology. Special thanks to Brigitte Mary for her administrative assistance. Also, I would also like to thank all the past and present members of Seidah's laboratory for their help, support, and positive energy.

I would also like to honorably acknowledge my committee members: Dr. Nicole Francis, Dr. Robert Day, and Dr. Dieter P. Reinhardt as well as our collaborator: Dr. Martin Sauvageau for his valuable inputs to the project.

Finally, I would like to express my acknowledgment to my family and all my friends for their encouragement, support, and motivation.

Contribution of Authors

Dr. Nabil G. Seidah (supervisor) and Sahar Mikaeeli (student) conceived of the presented idea and developed the theory. Dr. Nabil G. Seidah encouraged Sahar Mikaeeli to investigate and supervised the findings of this work and this project.

Sahar Mikaeeli carried out all the experiments, wrote the whole manuscript (chapter 1 to 4 and other parts of the thesis) with editorial input of Dr. Nabil G. Seidah and Both authors contributed to the final version of the manuscript.

Sahar Mikaeeli developed the theoretical formalism, performed the analytic calculations, contributed to sample preparation, contributed to the interpretation of the results with the help of Dr. Nabil G. Seidah, and designed the figures.

Preface

This dissertation is submitted for the degree of Master of Science at McGill University, faculty of Medicine, division of Experimental Medicine. The research was conducted under the supervision of Dr. Nabil G. Seidah in the Laboratory of Biochemical Neuroendocrinology at the Clinical Research Institute of Montreal (IRCM), Montreal.

It has been prepared in accordance with the guidelines for a “Traditional Monograph Thesis” and contains four chapters: I) Introduction, objectives and literature review, II) experimental procedures, III) results, and IV) discussion and future perspectives. This work has never been published before.

Table of Contents

Chapter 1:	23
1.1. Focus	23
1.2. Antisense oligonucleotides (ASOs), their structure and mechanism of action:	23
1.3. Non-alcoholic fatty liver disease (NAFLD)	23
1.3.1. <i>Clinical aspects of NAFLD</i>	24
1.3.2. <i>Risk factors of NAFLD</i>	25
1.3.3. <i>The genetic basis of NAFLD</i>	27
1.4. Triglycerides	29
1.4.1. <i>De novo biosynthesis of triglycerides</i>	31
1.4.2. <i>Dietary Triglyceride (exogenous Triglyceride supply) and its absorption</i>	31
1.4.3. <i>The importance of Triglyceride homeostasis and epidemiological studies (or its association with NAFLD)</i>	32
1.5. VLDL secretion	34
1.6. Lipoproteins and apolipoproteins	36
1.7. Post-translational modifications	38
1.8. Proprotein convertases family (PCs) and their discovery	40
1.8.1. <i>General structures, mechanism of action and subcellular localization of the PCs</i>	41
1.8.2. <i>Proprotein convertase members and their substrates</i>	42
1.9. Proprotein convertase subtilisin/kexin type 7 (PCSK7), its structure, biosynthesis, and physiological importance	45
1.9.1. <i>PC7 association with NAFLD</i>	47
1.10. Transmembrane 6 superfamily 2 protein (TM6SF2), its structure, biological function, and association with NAFLD	48
Hypothesis and Objectives.	49
Chapter 2:	53
Material & methods.	53
2.1. Reagents and Plasmids	53
2.2. The design of ASOs	53
2.3. Cell culture and cDNA transfections	55
2.4. Western blotting	55
2.5. Quantitative real-time PCR	55
2.6. Cell viability assay (MTS)	56
2.7. Flow Cytometry (FACS)	56

2.8. Oil Red O staining.....	56
Chapter 3:.....	58
Results.....	58
3.1 Design of ASOs to inhibit PC7 in human and mouse	58
3.2. Fluorescence-activated single-cell sorting (FACS) results showed high transfection efficiency of ASOs	58
3.3 Cell viability assay (MTS) showed a high percentage of cell viability after treatment with ASOs in both human and mouse cell lines.....	61
3.4. Human ASOs against the PCSK7 gene, showed a great reduction of PC7 protein levels and mRNA levels after 72 hours	62
3.5. Mouse ASOs against the PCSK7 gene, showed a great reduction of PC7 protein levels and mRNA levels after 72 hours	64
3.6. The IHH cells exhibit a highly significant reduction in the number of lipid droplets after 120 hours of treatment which ASO7	65
3.7. The FL83B cells exhibit a highly significant reduction in the number of lipid droplets after 66 hours of treatment which ASO7	67
3.8. Defining the relationship between the proteins PC7 and TM6SF2 using <i>in vitro</i> assays.....	68
3.9. TM6SF2 enhances the degradation of PCSK7 but not the ProPCsk7 in both HepG2 and IHH cell lines.....	70
3.10. TM6SF2 does not affect the levels of ER-localized PC7-D188G (only expresses proPC7) ...	71
3.11. The absence of PC7 does not affect the mRNA and Protein levels of TM6SF2	71
3.12. The protein and mRNA levels of PC7 significantly decreased in the absence of TM6SF2 in IHH cells using siRNAs to TM6SF2	71
Chapter 4:.....	73
General discussion and future perspectives.....	73
References:.....	78

List of Figures:

<i>Figure 1. The progressive stages of NAFLD</i>	25
<i>Figure 2. Clinical features of cirrhosis</i>	26
<i>Figure 3. Pathogenesis of nonalcoholic fatty liver disease (NAFLD)</i>	29
<i>Figure 4. An overview of TG-rich lipoproteins (TRL) metabolism</i>	34
<i>Figure 5. An overview of the four pathways involved in the homeostasis of lipids in the liver</i>	36
<i>Figure 6. Inhibition of ApoB and MTP by antisense oligonucleotides (ASOs)</i>	38
<i>Figure 7. Lipoprotein classification</i>	40
<i>Figure 8. primary structures of proprotein convertase family members</i>	42
<i>Figure 9. Zymogene processing of Pro-PC7 to PC7</i>	48
<i>Figure 10. The Proposed model for the TM6SF2 role in lipidation of VLDL particles</i>	50
<i>Figure 11. Schematic of designed ASOs on different exons on PCSK7 gene</i>	58
<i>Figure 12. Cell Viability results by FACS</i>	60
<i>Figure 13. mRNA levels of PC7 in four different cell lines by qPCR</i>	61
<i>Figure 14. Cell viability measured using MTS assay</i>	62
<i>Figure 15. PC7 protein and mRNA levels after transfection with human ASOS</i>	63
<i>Figure 16. PC7 mRNA levels after transfection with Mouse ASOS number 6, 7, and 8</i>	64
<i>Figure 17. Oil Red O results from hASO7 transfection in IHH cells</i>	66
<i>Figure 18. Oil Red O results from mASO7 transfection in FL83B cells</i>	67
<i>Figure 19. Human TM6SF2 protein sequence</i>	68
<i>Figure 20. Co-expressing PC7WT cDNA with TM6SF2-WT/TM6SF2-E167K/TM6SF2-S165.E</i>	69

Figure 21. Co-expressing PC7D-188G cDNA with TM6SF2-WT/TM6SF2-E167K/TM6SF2-S165E. 70

Figure 22. The TM6SF2 mRNA and protein levels 72 hours after PC7 inhibition using siRNAs (20nM) in IHH cells. 71

Figure 23. The PC7 mRNA and protein levels 72 hours after TM6SF2 inhibition using siRNAs (100nM) in IHH cells. 72

List of Tables

<i>Table 1. identified variants associated with NAFLD and other involved genes</i>	<i>31</i>
<i>Table 2. Lipoprotein classification</i>	<i>39</i>
<i>Table 3. The tissue expression and subcellular localization of PCs</i>	<i>44</i>
<i>Table 4. The human and mouse sequences of antisense oligonucleotides (ASOs)</i>	<i>53</i>

List of Abbreviations

aa: amino acids

AAV: adeno-associated virus

ACTH: adrenocorticotrophic hormone

ADAM: disintegrin- and-metalloproteinase

ADAM-TS4: disintegrin, and metalloprotease with thrombospondin motif 4

ASOs: antisense oligonucleotides

Apo (a): apolipoprotein (a)

Apo A-I: apolipoproteins AI

Apo A-II: apolipoprotein A-II

Apo A-IV: apolipoprotein A-IV

Apo A-V: apolipoprotein A-V

ApoA5: apolipoprotein A5

Apo B-48: apolipoprotein B-48

Apo B-100: apolipoprotein B-100

Apo C; apolipoprotein C

APOC3: apolipoprotein C3

Apo C-I: apolipoprotein C-I

Apo C-II: apolipoprotein C-II

Apo E: apolipoprotein E

ASGR1: asialoglycoprotein receptor 1

ATP: adenosine triphosphate

BDNF: brain-derived neurotrophic factor

7B2: neuroendocrine protein 7B2

ChREBP: carbohydrate regulatory element-binding protein

CASC4: cancer susceptibility candidate 4

cDNAs: complementary deoxyribonucleic acids

CD36: cluster of differentiation 36

CNS: central nervous system

COP1: constitutive photomorphogenic-1

CO₂: carbon dioxide

CREB4: cAMP response element-binding protein

CRD: Cys-rich domains

SOCS3: cytokine signaling 3

DAPPI: desorption atmospheric pressure photoionization

DNL: de novo lipogenesis

DEAF-1: deformed epidermal autoregulatory factor 1

DHAP: dihydroxyacetone phosphate

DNAs: deoxyribonucleic acids

DMEM: Dulbecco's Modified Eagle Medium

EMEM: Eagle's Minimum Essential Medium

EDTA: ethylenediaminetetraacetic acid

ER: endoplasmic reticulum

FAM20C: golgi associated secretory pathway kinase

FATPs: fatty acid transport proteins

FAO: fatty acid oxidation

FATP: fatty acid transport proteins

FBS: fetal bovine serum

FL1: green fluorescence

FL83B: Mouse hepatocytes

FACS: Flow Cytometry

FAM: fluorescent probe

FSC: forward scatter

FFAs: free fatty acids

F12K: Kaighn's Modification of Ham's F-12

GalNAc: N-acetyl galactosamine

GWAS: Genome-wide association study

GLP1, GLP2: glucagon-like peptide 1 & 2

GCKR: glucokinase regulator

G3P: glycerol-3-phosphate

GOF: gain-of-function

GDF11: growth differentiation factor 11

GH: growth hormone

GHRH: growth hormone-releasing hormone

HSPGs: heparan sulfate proteoglycans

HepG2: human hepatocellular carcinoma

HGFR: hepatocyte growth factor receptor

HDL: high-density lipoproteins

HK293: human embryonic kidney 293

HTN: systemic hypertension

HuH7: human liver cell line

IKK β : inhibitor of nuclear factor kappa B [NF- κ B]

IGF-1R: insulin-like growth factor 1 receptor

IHH: immortalized human hepatocytes

IDT: Integrated DNA Technologies

IDLs: Intermediate-density lipoproteins

IL-6: interleukin-6

IL-1 β : interleukin-1 β

IGF2: Insulin-like growth factor-2

KO: knockout

KW: knockdown

L1CAM: L1 cell adhesion molecule

LDs: lipid droplets

LPL: lipoprotein lipase

LYPLAL1: lysophospholipase-like 1

MCH: melanin-concentrating hormone

MBOAT7: Membrane-bound O-acyltransferase domain containing 7

MTP: microsomal triglyceride transfer protein

mRNA: messenger ribonucleic acid

MMP14: metalloproteinases

MTS: Aqueous One Solution Cell Proliferation Assay

MetS: metabolic syndromes

NaCl: sodium chloride

NCAN: Neurocan

ND: normal diet

NF- κ B: nuclear factor – kappaB

NAFLD: non-alcoholic fatty liver disease

NASH: Non-alcoholic steatohepatitis

PACAP: pituitary adenylyl cyclase-activating peptide

PACE4: paired basic amino acid cleaving enzyme 4

PCs: Proprotein convertases family

PCOS: polycystic ovary syndrome

PNPLA3: patatin-like phospholipase domain containing 3

POMC: pro-opiomelanocortin

PPAR α : peroxisome proliferator-activated receptor alpha

PPAR γ : peroxisome proliferator-activated receptor gamma

PTMs: Post-translational modifications

pcDNA3.1: plasmid complementary deoxyribonucleic acid 3.1 (expression vector)

PC1: proprotein convertase 1

PC2: proprotein convertase 2

PC4: proprotein convertase 3

PC5: proprotein convertase 5

PC7 proprotein convertase #7 (PC7) gene (*PCSK7*)

PCR: polymerase chain reaction

PPP1R3B: regulatory subunit 3B

PCSK9: proprotein convertase subtilisin kexin 9

PPAR- γ : peroxisome proliferator-activated receptor gamma

ProPC: Inactive zymogens

pH: power of hydrogen

PS: phosphonothioate

PIRES: a mammalian expression vector

proNGF: initially translated neurotrophic nerve growth factor

proPACAP: initially translated pituitary adenylate cyclase-activating polypeptide

PTPRM: protein Tyrosine phosphatase receptor type M

PVDF: polyvinylidene fluoride or polyvinylidene difluoride

ROS: reactive oxygen species

RGMA: repulsive guidance molecule BMP co-receptor A

RIPA: radioimmunoprecipitation assay buffer

RISC: RNA-induced silencing complex

RNAs: ribonucleic acids

RNase H: ribonuclease H

SDS: sodium dodecyl sulfate

SDS-PAGE: sodium dodecyl sulfate-polyacrylamide gel electrophoresis

SGs: secretory granules

SSC: side scatter

siRNAs: small interfering RNA

SNP: single-nucleotide polymorphism

SREBP1c: sterol regulatory element-binding protein 1c

SKI-1: subtilisin kexin isozyme 1

T2DM: type 2 diabetes mellitus

TRLs: (TG)-rich lipoproteins

TNF- α : tumor necrosis factor-alpha

TGF β : tumor necrosis factor-beta

TfR1: transferrin receptor 1

TGN: Trans-Golgi network

TM6SF2: transmembrane 6 Superfamily Member 2

TRIB1: tribble pseudokinase 1

TG/ TAG: Triacylglycerides

Tris-HCl: tris hydrochloric acid

VLDL: very low-density lipoprotein

WT: wild type

Chapter 1:

Introduction.

1.1. Focus

The main focus of this master's thesis is the study of the inhibition of the proprotein convertase #7 (PC7) gene (*PCSK7*) using antisense oligonucleotides (ASOs) *in vitro*, as a potentially new therapeutic approach for the treatment of non-alcoholic fatty liver disease (NAFLD). In addition, we evaluated the possible *in vitro* interaction between PC7 and the transmembrane 6 Superfamily Member 2 (TM6SF2), known to play a key role in NAFLD.

1.2. Antisense oligonucleotides (ASOs), their structure and mechanism of action:

Antisense oligonucleotides (ASOs) were discovered for the first time by Zamecnik and Stephenson [1,2]. They are single-stranded sequences of deoxyribonucleic acids (DNAs) or ribonucleic acids (RNAs) of 16-25 bases in length designed to target a specific messenger ribonucleic acid (mRNA) related to a gene of interest by the Watson-Crick base pairing system for silencing that gene. After binding to mRNA, the DNA-RNA hybrid will be recognized by endonuclease ribonuclease H (RNase H) that cleaves the mRNA strand resulting in the knockdown of the gene [3]. The ASOs can be modified in different ways to be more stable and efficient. One of the modifications of ASOs is the addition of a phosphorothioate (PS) linkage. This modification results in better binding to plasma proteins and subsequently enhanced uptake by cells and tissues. Also, this protects the ASOs against nucleases and improves the degradation of the DNA-RNA duplex by RNase H [4,5]. Another chemical modification is the addition of 2'-O-methoxyethyl groups to the ASOs. This

modification also protects the ASOs against nuclease degradation and the reduces host immune response (Figure1) [6].

There are many advantages in using ASOs instead of similar silencing tools such as siRNAs and miRNAs. Indeed, the ASOs are single stranded and small, making them appropriate for additional modifications and delivery. Also, ASOs target nuclear and cytoplasmic RNAs since they do not need to recruit the RNA-induced silencing complex (RISC), which is in the cytoplasm. These advantages make the ASOs as powerful therapeutic tools for the treatment of diseases. The successful application of ASOs for the treatment of central nervous system (CNS) disorders during recent years enhanced the focus of the pharmaceutical industry on the development of ASOs for the treatment of other disorders [3].

1.3. Non-alcoholic fatty liver disease (NAFLD)

Nonalcoholic fatty liver disease (NAFLD) is a systemic condition which is associated with metabolic, cardiovascular, and increased risk of hepatic cancer [7,8]. It is also highly associated with type 2 diabetes and insulin resistance. Non-alcoholic steatohepatitis (NASH) is a more progressive condition which is associated with steatosis, inflammation and can occur in the presence or absence of fibrosis [9]. In some patients, this condition can progress to even more severe conditions such as cirrhosis and tissue scarring, leading to liver failure with a mortality rate much higher than Non-alcoholic steatohepatitis (NASH). The most severe late and irreversible condition is hepatocellular carcinoma. Currently, there is not any approved treatment for this disease and the liver transplantation is the only available treatment for only patients with progressed hepatocellular carcinoma. [10,11] (figure 1).

Non-alcoholic fatty liver disease (NAFLD) is a prominent cause of liver disease worldwide, affecting ~35% of humans. It is most prevalent in the Middle East and South America and is less prevalent in Africa [12-15]. NAFLD affects up to 30% of the European population. In the United States, it is expected that the affected people will increase from ~25% in 2015 to 30% of the population in 2030 [13].

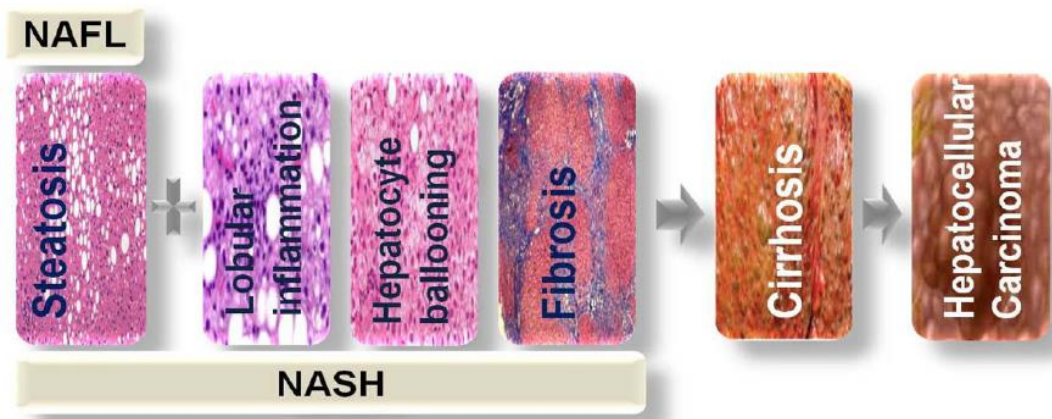


Figure 1. The progressive stages of NAFLD [16].

1.3.1. Clinical aspects of NAFLD

Usually, in the early stages of NAFLD patients are asymptomatic. This lack of symptoms and appropriate diagnostic tools during the early stages of NAFLD renders very difficult the effective management of the disease. Patients may show an increased level of some markers in the blood such as liver enzymes, dyslipidemia, and abnormal glucose metabolism [17]. Likewise, they may complain about abdominal pain in the right upper quadrant, fatigue, and obesity.

Hepatomegaly or enlarged liver can be recognized during physical examination [18]. In the NAFLD condition hepatic triglyceride content is 5.5% or more. Some metabolic syndromes can be associated with NAFLD including endocrine diseases, such as polycystic ovary syndrome

(PCOS), hypothyroidism, hypogonadism, and growth hormone (GH) deficiency [19,20]. Therefore, for a more accurate diagnosis of this disease, signs related to metabolic syndromes should be considered such as hypertension and hyperlipidemia, diabetes mellitus or T2DM, obesity, and increased serum aminotransferase levels [21,22-26]. Increased blood lipids such as cholesterol and triglycerides and other serum biomarkers are also efficient diagnostic tools besides imaging, however, NAFLD patients mostly do not show any biochemical abnormalities. [27,28] [29,30,31,32].

Almost 20% of patients with NAFLD progress to more acute fibrosis and cirrhosis [33] and show clinical consequences that are caused by lipid storage in the liver. At this stage, there are some manifestations including *spider naevi* (red spots with radiating extensions), palmar erythema (reddening of the palms), prominent abdominal veins, gynecomastia (enlargement of male breast tissue), jaundice (yellowing of the eyes and skin), ascites (fluid in the abdominal cavity), splenomegaly (enlarged spleen), nail changes (e.g., clubbing) and asterixis [34]. (figure 2).

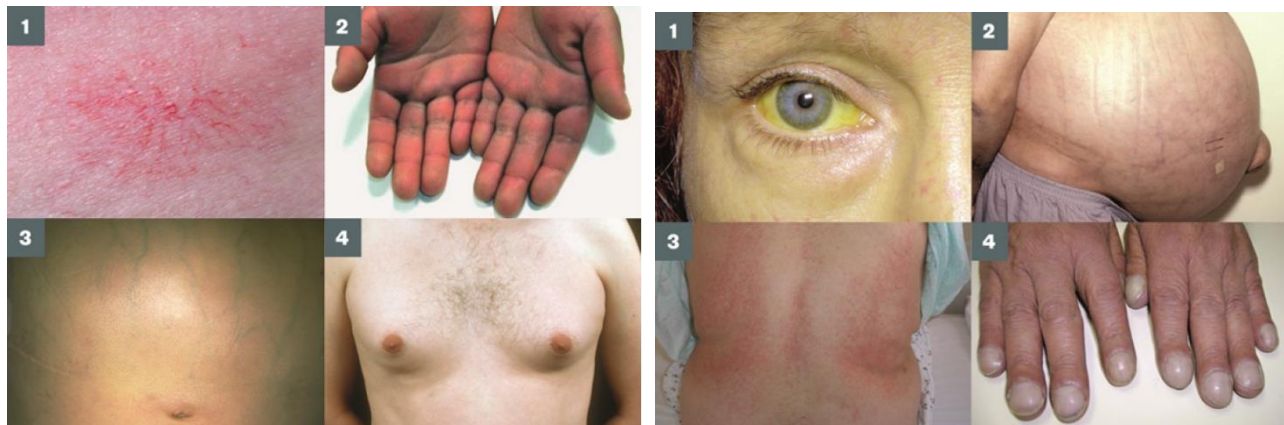


Figure 2. Clinical features of cirrhosis (left). Clinical features of decompensated cirrhosis (right)

1.3.2. Risk factors of NAFLD

The pathogenesis of NAFLD is unclear. But it is suggested that genetic variations and environmental risk factors can lead to the development of NAFLD. According to the "multiple hit" hypothesis, many hits cumulatively lead to the development of NAFLD [35]. Some of these hits include insulin resistance, hormones secreted from the adipose tissue, nutritional factors, gut microbiota, and genetic and epigenetic factors [35–38].

On the other hand, the metabolic syndromes (MetS) such as obesity hyperglycemia, dyslipidemia, and systemic hypertension (HTN) are the most prominent risk factors for NAFLD [39]. Also, Obesity is one of the most significant causes leading to free fatty acids (FFAs) penetration of the liver [40,41]. Over-consumption of iron, cholesterol, and refined sugars used in processed foods increases the risk of NAFLD development. Further, diabetes mellitus and conditions associated with insulin resistance are important risk factors in NAFLD [42]. More than 75% of patients with type 2 diabetes have NAFLD. The risk of progressing to NASH is higher in patients with both diabetes and NAFLD in comparison with those with NAFLD only [43-45].

In the liver, FFAs are sorted to three pathways including beta-oxidation in mitochondria, packaging in very low-density lipoprotein (VLDL) through apolipoprotein B (ApoB) to be secreted into the blood, and biosynthesis of triglycerides [46]. The uptake of these FFAs by hepatic tissue is assisted by fatty acid transport proteins (FATPs) and cluster of differentiation 36 (FAT/CD36) (fatty acid translocase). In patients with NAFLD elevated levels of these proteins has been reported [47,48].

Fat accumulation or triglyceride storage in lipid droplets in hepatocytes lead to steatosis, which is a reversible stage [49]. This could be due to diet, gut microbiota, genetic factors, and *de novo* lipogenesis through up-regulation of some lipogenic transcription factors such as sterol regulatory binding protein-1c (SREBP1c), carbohydrate-responsive element-binding protein (chREBP), and peroxisome proliferator-activated receptor gamma (PPAR- γ) [50, 51,52,53].

Steatosis leads to upstream inactivation of inhibitor of nuclear factor kappa B [NF- κ B] (IKK β) *via* reduced peroxisome proliferator-activated receptor alpha (PPAR α) activity, resulting in enhanced signaling by the transcription factor nuclear factor – kappa β (NF- κ β). In turn, this would increase the production of inflammatory cytokines such as tumor necrosis factor-alpha (TNF- α), interleukin-6 (IL-6), and interleukin-1 β (IL-1 β), followed by activation of Kupffer cells (resident hepatic macrophages) [53] thereby increasing the inflammation occurring in NASH [54].

Also, TNF- α and IL-6 up-regulate the Suppressor of cytokine signaling 3 (SOCS3) leading to hepatic insulin resistance [55, 56]. Likewise, steatosis is a cause of lipotoxicity and results in organelle failure (mitochondria and endoplasmic reticulum) [57, 58]. When the mitochondria cannot function properly, it enhances fatty acids oxidation leading to oxidative stress because of elevated production of reactive oxygen species (ROS) [59, 60] and hence increased formation of free radicals (Figure 3) [61].

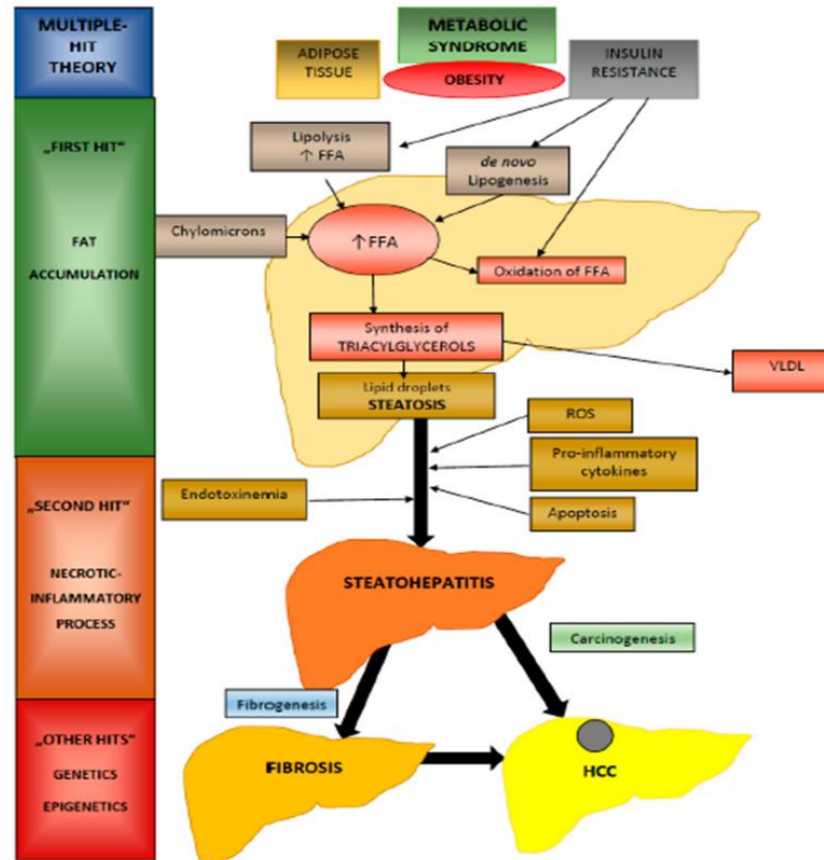


Figure 3. Pathogenesis of nonalcoholic fatty liver disease (NAFLD) [49].

1.3.3. The genetic basis of NAFLD

There are many genetic factors identified concerning the increased risk of NAFLD and NASH. A Genome-wide association study (GWAS) [62] showed that the most evident genetic association is a single-nucleotide polymorphism in the patatin-like phospholipase domain containing 3 (*PNPLA3*) gene [63]. This gene encodes lipase enzyme. The Lipase regulates lipolysis of lipid droplets [64,65] and hydrolyzes the triacylglycerols in hepatocyte and adipocytes, respectively [64, 66]. Based on previous studies, there is a relevance between the *PNPLA3* I148M variant (rs738409) (loss of lipase activity of *PNPLA3*) with increased liver fat content and NAFLD [64].

GWAS also revealed another gene highly associated with NAFLD, called transmembrane 6 superfamily member 2 (*TM6SF2*), which is localized in the endoplasmic reticulum (ER). The single-nucleotide polymorphism (SNP) E167K (rs58542926 C/T), causes a loss-of-function of *TM6SF2* protein by destabilizing the protein. There is a correlation between this SNP and elevated hepatic triglyceride content, increased amounts of aminotransferases, reduced levels of triglycerides and LDL-cholesterol in serum, and increased steatosis [67].

Neurocan (*NCAN*-rs2228603), protein phosphatase 1, regulatory subunit 3B (*PPP1R3B*-rs4240624), glucokinase regulator (*GCKR*-rs780094), and lysophospholipase-like 1 (*LYPLAL1*-rs12137855) are other variants identified by GWAS associated to NAFLD [68].

There are several other genes involved in NAFLD. Apolipoprotein C3 (*APOC3*) gene encodes a protein component of triglyceride (TG)-rich lipoproteins (TRLs) and inhibits the lipolysis of these TRLs, by blocking the lipoprotein lipase activity. The Glucokinase regulator (*GCKR*) gene encodes a protein that inhibits glucokinase in liver cells. Membrane-bound O-acyltransferase domain containing 7 (*MBOAT7*) gene encodes a member of the membrane-bound O-acyltransferases family of membrane proteins with acyltransferase activity. The tribble pseudokinase 1 (*TRIB1*) gene encodes an adapter protein that interacts with COP1 ubiquitin ligase and leads to protein degradation (Table 1) [69].

Table 1: identified variants associated with NAFLD and other involved genes.

Genes and variants involved in NAFLD	References
patatin-like phospholipase domain containing 3 (<i>PNPLA3</i> -rs738409)	[62-66]
transmembrane 6 superfamily member 2 (<i>TM6SF2</i> - rs58542926)	[67]
Neurocan (<i>NCAN</i> -rs2228603)	[68]
protein phosphatase 1	[68]
regulatory subunit 3B (<i>PPP1R3B</i> -rs4240624)	[68]
glucokinase regulator (<i>GCKR</i> -rs780094)	[68]
lysophospholipase-like 1 (<i>LYPLAL1</i> -rs12137855)	[68]
Apolipoprotein C3 (<i>APOC3</i>)	[69]
The Glucokinase regulator (<i>GCKR</i>)	[69]
Membrane-bound O-acyltransferase domain containing 7 (<i>MBOAT7</i>)	[69]
The tribble pseudokinase 1 (<i>TRIB1</i>)	[69]

1.4. Triglycerides

Triacylglycerides (TAG; triglycerides, TG) are stored forms of fatty acids in cells that provide energy and are involved in cellular metabolism. Adipocytes in adipose tissue are the main tissue involved in TAG storage. All eukaryotes and few prokaryotes synthesize triacylglycerols. The liver, intestines, and adipose tissue are active in the synthesis and storage of TAGs, which are stored in lipid droplets.

1.4.1. *De novo biosynthesis of triglycerides*

There are three main pathways for the biosynthesis of triglycerides including the glycerol-3-phosphate (G3P) pathway (or Kennedy pathway), the dihydroxyacetone phosphate (DHAP) pathway, and the monoacylglycerol pathway. The Kennedy pathway, first described by Eugene Kennedy and colleagues in the 1950s, is responsible for the synthesis of more than 90% of the liver triglycerides. The DHAP pathway which uses the DHAP produced from glycolysis is the

major triglyceride synthesis pathway in the liver under insulin stimulation conditions. The monoacylglycerol pathway uses dietary fatty acids for the biosynthesis of triglycerides in enterocytes of the small intestine.

Although triacylglycerols are crucial for the normal physiology and function of the body, the excess accumulation of them results in NAFLD. Therefore, it can be a target for designing drugs for the treatment of NAFLD.

After endogenous synthesis of TGs, they enter two pathways depending on the cell condition. They can be stored as cytosolic lipid droplets, which consist of a core of triglycerides and cholesterol esters surrounded by a phospholipid monolayer, [70-76] or they can be transported to the ER and packaged into very-low-density lipoprotein (VLDL) particles for secretion [77,78]. These VLDL particles are made of a core of triglycerides surrounded by apolipoprotein B-100 (ApoB100) (instead of about-48), apolipoprotein C-I (ApoC-I), apolipoprotein C-II (ApoC-II), apolipoprotein C-III (ApoC-III), and apolipoprotein E (ApoE). After secretion, VLDLs hydrolyzed by lipoprotein lipase (LPL), results in the production of smaller remnant VLDL particles, which are high in cholesterol esters and then intermediate-density lipoproteins (IDLs). Some IDL particles are internalized in the liver, and the rest undergo more catabolism by LPL leading to the production of low-density lipoprotein particles (LDL), which can further be taken up by LDL receptors to provide cholesterol for hepatic cells. [79, 80, 81, 82-84]

1.4.2. Dietary Triglyceride (exogenous Triglyceride supply) and its absorption

In the exogenous pathway, dietary triglycerides and cholesterol are absorbed by enterocytes after hydrolyzing in the intestinal lumen. In this step, first, the ingestion will occur in the intestine including emulsification of the absorbed lipids which makes them suitable for hydrolysis. Then,

triglycerides and cholesterol undergo re-esterification in the mucosal cells in the intestine where they will be coupled with different kinds of apoproteins and phospholipids and will be packaged into chylomicrons [77, 78, 84-87]. chylomicrons are large spherical lipoproteins that contain a phospholipid monolayer with free cholesterol and apolipoprotein B48 (apoB48 and massive TG core (80-95%). They are formed for the secretion of triglycerides into the bloodstream to peripheral tissues and the liver. Other apolipoproteins ApoC-II, ApoC-III, and ApoE are required for the secretion of Chylomicrons. Also, some other kinds of apolipoproteins can be found on them including apolipoproteins AI (ApoAI), apolipoproteins AIV (ApoAIV).

After the entry of chylomicrons into circulation, they bind lipoprotein lipase (LPL) leading to their hydrolysis in the luminal surface of the capillaries. The LPL must be activated by ApoC-II to be able to do the hydrolysis. Likewise, ApoC-III, apolipoproteins A5 (ApoA5), and angiopoietin-like proteins 3 and 4 regulate ApoC-II function.

The hydrolysis of chylomicrons leads to the production of free fatty acids which will be stored in adipocytes or will undergo oxidation to be used as energy in skeletal muscle cells or myocardial myocytes. Also, chylomicron remnants will be formed from the hydrolysis of chylomicrons. They are high in cholesterol and contain ApoE, ApoB-48, and ApoC-III. These chylomicron remnants will further bind to the liver-specific receptors called LDL receptors through their ApoE and will enter hepatocytes to be degraded in lysosomes (Figure4) [78,79].

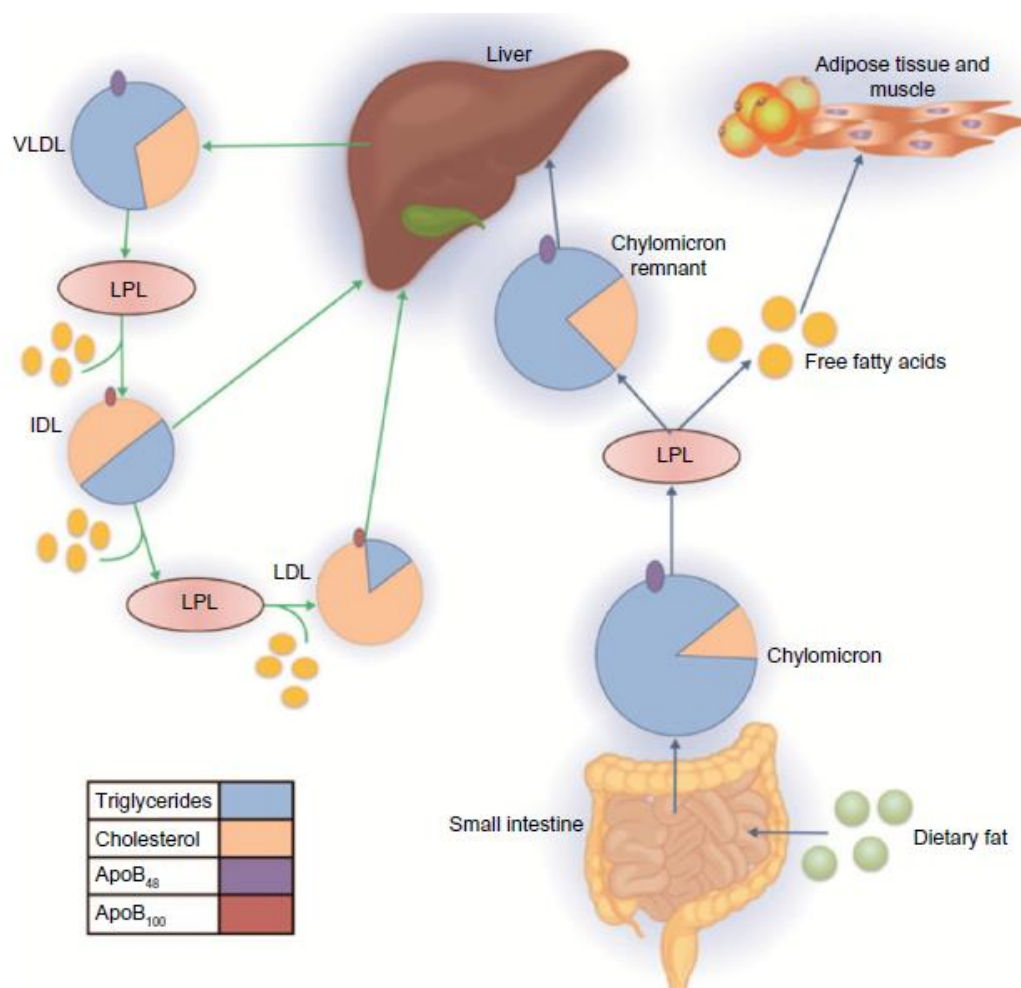


Figure 4. An overview of TG-rich lipoproteins (TRL) metabolism [78].

1.4.3. The importance of Triglyceride homeostasis and epidemiological studies (or its association with NAFLD)

The liver is a prominent regulator of lipid homeostasis and leads to a balance between lipid acquisition and lipid disposal pathways. These pathways include uptake of circulating lipids, de novo lipogenesis (DNL), fatty acid oxidation (FAO), and export of lipids in very-low-density

lipoproteins (VLDL). These pathways are also regulated by hormones and transcription factors. Any interruption in balancing between these four mechanisms results in lipid accumulation in the hepatocytes and NAFLD (Figure 5) [88,89].

The uptake of circulating lipids is mediated by some fatty acid transporters on the plasma membrane of the hepatocyte. The fatty acid transport proteins (FATP) are a group of six isoforms in which only FATP2 and FATP5 are in the liver to facilitate uptake of lipids. Another fatty acid transporter is the cluster of differentiation 36 (CD36), that mediates the transport of long-chain fatty acids. finally, caveolins represent cytosolic proteins regulating endocytosis of cargoes, which are regulated by PPAR γ [90-93].

De novo lipogenesis (DNL) is another mechanism involved in lipid regulation. DNL is regulated by two transcription factors including the sterol regulatory element-binding protein 1c (SREBP1c) and the carbohydrate regulatory element-binding protein (ChREBP) [94-96].

Oxidation of fatty acids occurs in mitochondria, to produce ATP as a source of energy. This mechanism is regulated by PPAR α . The oxidation of very-long-chain fatty acids occurs in peroxisomes and in some conditions like NAFLD when there is a significant amount of lipids inside the cytoplasm, cytochromes will contribute through ω -oxidation. Oxidation of fatty acids in peroxisomes, and cytochromes results in producing a great number of reactive oxygen species (ROS), which could lead to inflammation [97, 98].

Lipid export in another pathway which can reduce the amount of lipid inside the cells by packaging them into VLDL particles [86].

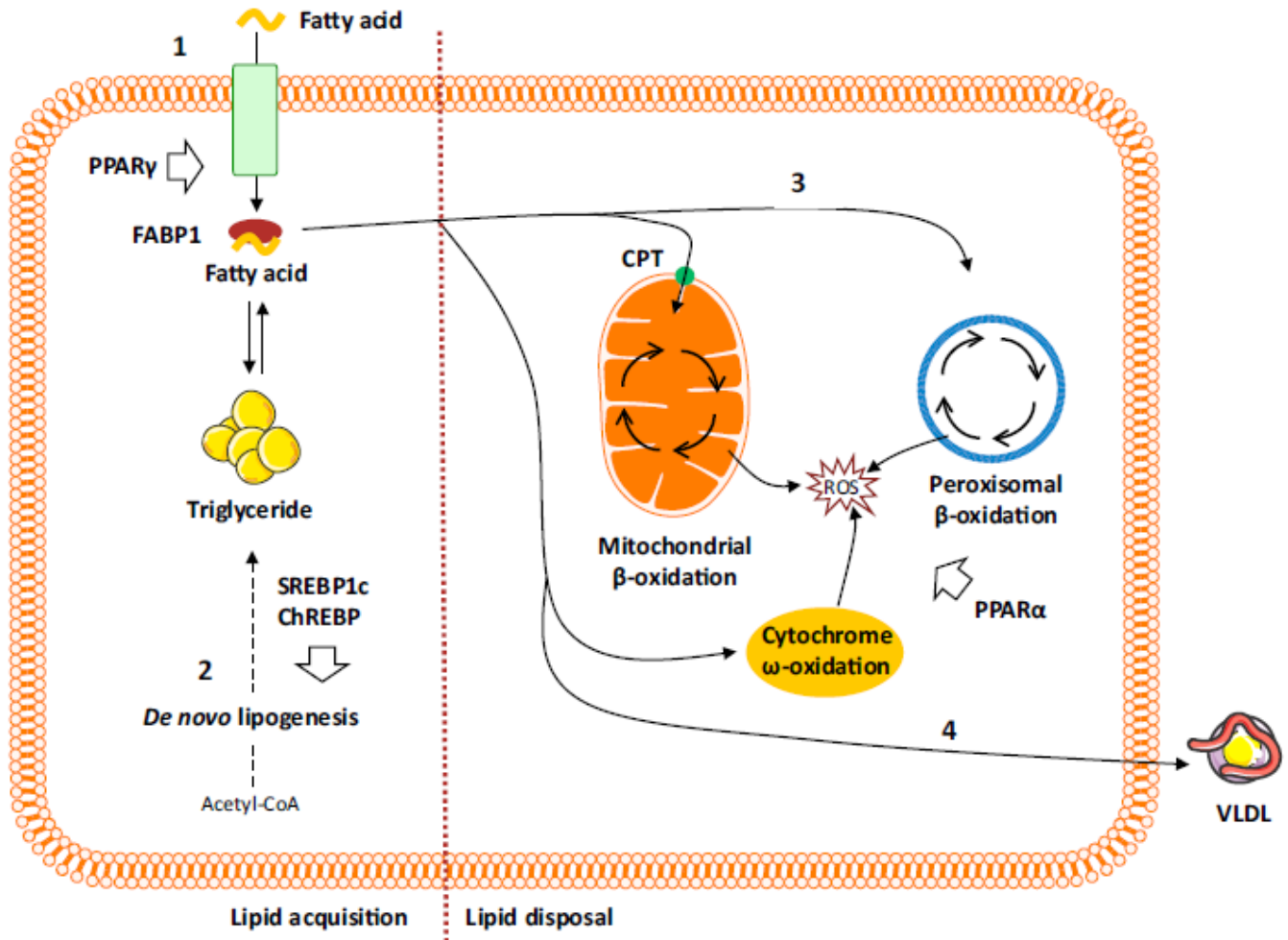


Figure 5. An overview of the four pathways involved in the homeostasis of lipids in the liver. 1) Uptake of circulating lipids 2) De novo lipogenesis 3) Oxidation of fatty acids 4) Lipid export [86].

1.5. VLDL secretion

VLDL lipidation occurs in the endoplasmic reticulum, where microsomal triglyceride transfer protein (MTP) translocates the TGs from lipid droplets across the ER and transfers them to apolipoprotein B100 (ApoB100). The nascent VLDL particle is then transferred to the Golgi apparatus where mature VLDL particles are formed by more lipidation ultimately leading to their secretion outside the cell, with ApoB100 as the only protein constituent. The TG content is

affecting the size and secretion of VLDLs [99, 100]. On the other hand, MTP is a key protein for the lipidation of ApoB100 and regulates its catabolism since in its absence ApoB is degraded by the proteasome. Therefore, the reduced levels of MTP or ApoB dramatically decrease VLDL secretion, resulting in steatosis and NAFLD. During an investigation, antisense oligonucleotides (ASOs) were used to target MTP and apoB separately for silencing their related genes in mice. The results showed that the absence of apoB after 6 weeks did not result in steatosis but decreased the VLDL secretion while the absence of MTP leads to steatosis. They indicated that the absence of apoB results in accumulation of TG in the ER and after 3 weeks this upregulates ER stress leading to ER micro-autophagy followed by lysosome-directed fatty acid oxidation and finally prevention of steatosis [101, 102]. These results support that the apoB can be a promising target for the treatment of NAFLD (Figure 6).

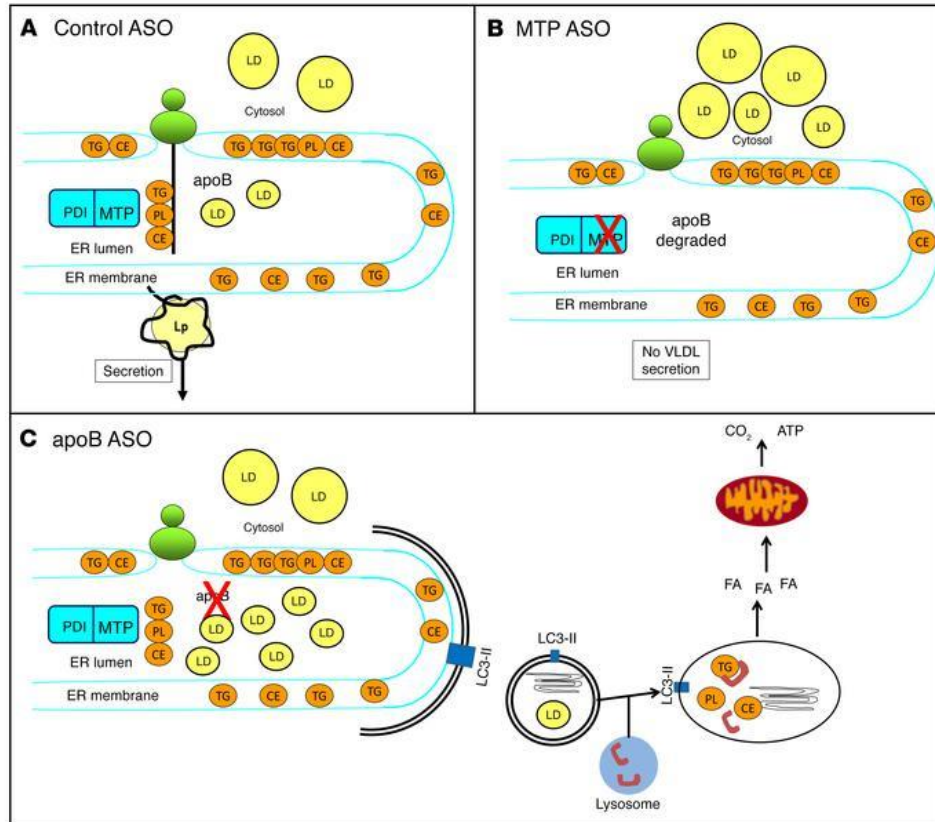


Figure 6. Inhibition of apoB and MTP by antisense oligonucleotides (ASOs) 1) In control, both the apoB and MTP are active 2) In MTP ASO-treated mice, absence of MTP results in steatosis 3) In apoB ASO-treated mice, the absence of apoB prevents steatosis after 6

1.6. Lipoproteins and apolipoproteins

Since lipids, such as cholesterol and triglycerides are not soluble in the water-based circulation system, they need to be packaged insoluble proteins called lipoproteins to be enable their transport through circulation [104]. Lipoproteins consist of a lipid core (cholesterol esters and triglycerides) which is quite hydrophobic surrounded by a hydrophilic phospholipid layer that contains free cholesterol and apolipoproteins. Apolipoproteins are specific proteins required for the assembly of lipids in lipoprotein particles. Indeed, they are divided into several subtypes including

apolipoproteins AI (Apo A-I), apolipoprotein A-II (Apo A-II), apolipoprotein A-IV (Apo A-IV), apolipoprotein A-V (Apo A-V), apolipoprotein B-48 (Apo B-48), apolipoprotein B-100 (Apo B-100), apolipoprotein C (Apo C), Apo C-II, Apo C-III, apolipoprotein E (Apo E), apolipoprotein (a) (Apo (a)). Further, these lipoproteins are classified into seven different groups based on their size, lipid composition, and apolipoproteins including chylomicrons, chylomicron remnants, very-low-density lipoproteins (VLDL), intermediate-density lipoproteins (IDL; VLDL remnants), low-density lipoproteins (LDL), high-density lipoproteins (HDL), and lipoprotein an LP(a) (Figure 7) (Table 2) [105, 106].

Table 2. Lipoprotein classification [105]

Lipoprotein	Density (g/ml)	Size (nm)	Major Lipids	Major Apoproteins
Chylomicrons	<0.930	75-1200	Triglycerides	Apo B-48, Apo C, Apo E, Apo A-I, A-II, A-IV
Chylomicron Remnants	0.930- 1.006	30-80	Triglycerides Cholesterol	Apo B-48, Apo E
VLDL	0.930- 1.006	30-80	Triglycerides	Apo B-100, Apo E, Apo C
IDL	1.006- 1.019	25-35	Triglycerides Cholesterol	Apo B-100, Apo E, Apo C
LDL	1.019- 1.063	18- 25	Cholesterol	Apo B-100
HDL	1.063- 1.210	5- 12	Cholesterol Phospholipids	Apo A-I, Apo A-II, Apo C, Apo E
Lp (a)	1.055- 1.085	~30	Cholesterol	Apo B-100, Apo (a)

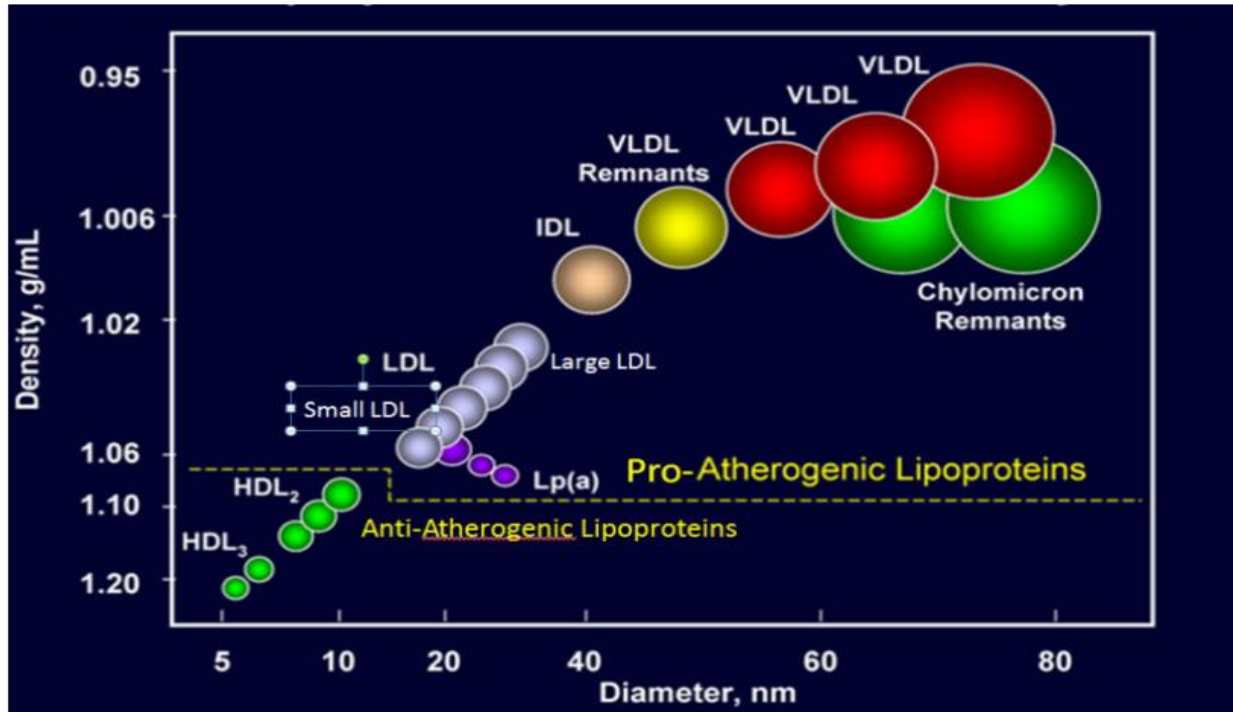


Figure 7. Lipoprotein classification [105].

1.7. Post-translational modifications

Post-translational modifications (PTMs) are reversible or irreversible covalent alterations generating modified proteins and enzymes. These transcriptional and post-transcriptional modifications explain the diverse range of almost 1 million proteins from only 22,000 genes in the human genome. Until now, around 200 PTMs have been identified, which are categorized into different types including, acetylation, methylation, phosphorylation, ubiquitination, glycosylation, nitrosylation, lipidation, and proteolysis. PTMs are very crucial for the appropriate function of cells by affecting the protein interactions, localization, and turnover. Among these modifications, proteolysis is an irreversible modification resulting in the cleavage of peptide bonds of proteins to activate or inactivate their function. There are five different groups of proteases including, serine,

cysteine, metallo, and threonine. Likewise, there are two subtypes for serine proteases including chymotrypsin-like (trypsin-like) and subtilisin-like proteases. the mammalian proprotein convertases are important members of serine proteases related to yeast kexin [106-112].

1.8. Proprotein convertases family (PCs) and their discovery

It was between 1989-1990 when the first mammalian proprotein convertases were discovered named PC1, PC2, and Furin. Interestingly, other members of this basic-amino acid specific protease family were later discovered including PC4, PC5, paired basic amino acid cleaving enzyme 4 (PACE4), and PC7. finally, the last two members including subtilisin kexin isozyme 1 (SKI-1) and proprotein convertase subtilisin kexin 9 (PCSK9) were discovered in 1999 and 2003, respectively [110, 113].

The mammalian proprotein convertases (PCs) belong to the secretory protease's family. The first seven PCs (PC1, PC2, furin, PC4, PC5, PACE4, and PC7) cleave the substrates at single or paired basic amino acid residues. The motif recognized by them is (R/K) X_n (R/K) ↓ where 'n' corresponds to 0,2,4 or 6 spacer amino acids and X can be any aa. Whereas the other two members (SKI-1/S1P and PCSK9) cleave at non-basic residues and they can recognize motif RX(L/V/I) X↓ where X and Z can be variable and VFAQ↓, respectively. It is important to note that PCSK9 has only one substrate, which is itself, and following its autocatalytic cleavage in the ER and secretion no longer acts as an active protease since it remains inhibited by its non-covalent interaction with its N-terminal inhibitory prodomain enzyme (Figure 8) [114, 115].

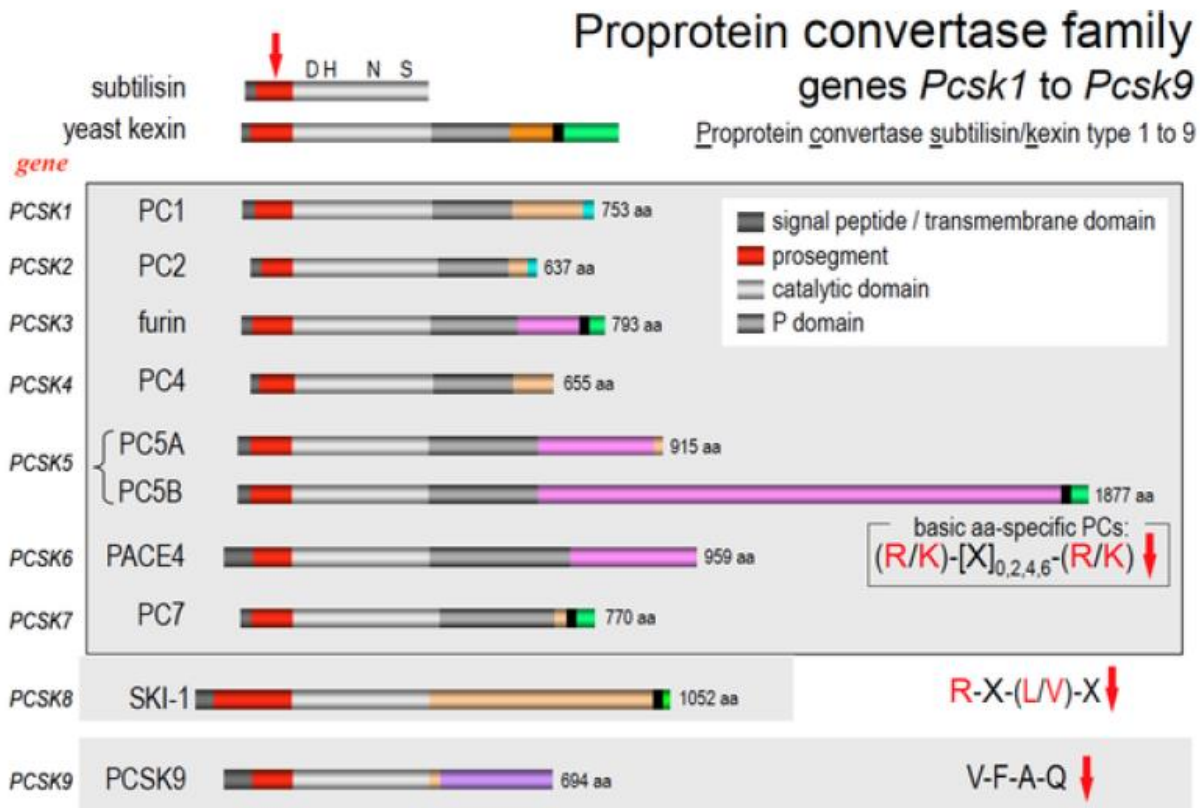


Figure 8. primary structures of proprotein convertase family members [115].

1.8.1. General structures, mechanism of action and subcellular localization of the PCs

The general structure of all PCs contains a signal peptide, pro-segment, catalytic domain, and C-terminal. Also, all of them have their unique sequences required for their localization and trafficking inside the cells. The catalytic domain of PCs includes Asp, His, and Ser residues along with the oxyanion hole Asn residue. Four convertases including furin, PC7, the isoform PC5B, and SKI-1 are type I membrane-bound proteins and the rest are soluble and are either packaged into dense-core granules like PC1 and PC2 or remain membrane bound (PC4) or are secreted into the extracellular space (PC5A, PACE4, and PCSK9). Also, some PCs have specific features which

are critical for their function or sub-cellular localization. Indeed, the soluble form of PC5A and PACE4 have similar Cys-rich domains (CRD), required for their proper interactions with other proteins, such as cell surface heparan sulfate proteoglycans (HSPGs). PCSK9 has a Cys-His rich domain (CHRD) which is essential for its intracellular trafficking and function. Finally, furin, PC5B, and PC7 contain a transmembrane domain anchoring them to membranes [113, 116].

The proprotein convertases undergo post-translation modifications allowing them to be targeted to their substrates in specific compartments. PCs initially are translocated in the ER as inactive zymogens (ProPC) where after their signal peptide cleavage they autocatalytically cleave their N-terminal pro-domain and are N-glycosylated. Cleavage of the PC-pro-segment is required for the protein to exit the ER as an inactive complex of the Pro-segment with the mature protein. Only after the pro-domain separates is the mature enzyme fully active. This can result from a second autocatalytic cleavage of the prodomain, e.g., in the medial Golgi for SKI-1, the TGN for furin, the cell surface for PC5 and PACE4 and early endosomes for PC7. PCSK9 is the only convertase that remains attached to its pro-segment and therefore never acts as a protease and only can cleave itself. Also, there is an exception for the PC2. The zymogen proPC2 exits the ER as a complex with its chaperone 7B2 and only in immature secretory granules does proPC2 get activated by autocatalysis. Only PC4 and PC7 separate from their prodomain without the need of a secondary autocleavage, a process likely regulated by calcium. Thus, active PCs occur in different subcellular locations: PC1 and PC2 in immature dense-core secretory granules (SGs), furin in the Trans-Golgi network (TGN), cell surface and endosomes, PC5A and PACE4 at the cell surface, PC7 within endosomes following its internalization for the cell surface, and SKI-1 in the *cis/medial* Golgi [115]. Tissue expression of PCs and their subcellular localization is shown in (Table 3) [115].

Table 3. The tissue expression and subcellular localization of PCs [115].

Proprotein convertase	Tissue distribution	Subcellular localization	Secretion
PC1	Neuroendocrine	Acidic regulated secretory granules	Secreted
PC2			
Furin	Ubiquitous	TGN, cell surface, endosomes	Shed
PC4	Germinal	Cell surface?	Shed
PC5	Widespread: adrenal cortex, intestine, kidney, ovary	Cell surface, ECM	Secreted PC5A; shed PC5B
PACE4	Widespread: muscle, heart, pituitary, intestine, cerebellum, kidney	Cell surface, ECM	Secreted
PC7	Ubiquitous	TGN, cell surface, endosomes	Not secreted
SKI-1 (also known as S1P)	Ubiquitous	<i>cis</i> - and <i>medial</i> -Golgi	Not secreted
PCSK9	Liver, intestine, kidney	TGN, extracellular	Secreted

ECM, extracellular matrix; PACE4, paired basic amino acid cleaving enzyme 4; PC1, proprotein convertase 1; PCSK9, proprotein convertase subtilisin kexin 9; SKI-1, subtilisin kexin isozyme 1; TGN, *trans*-Golgi network.

1.8.2. Proprotein convertase members and their substrates

Investigations on different members of proprotein convertases revealed new insights about each of them. Also, each PC regulates a vast variety of mechanisms inside the cells through activation or inactivation of their substrate. Hence, we will go through a summary of each member.

PC1 and PC2: are mostly expressed in the neuroendocrine tissues. They have a complementary effect on each other and have their substrates in which some of them are similar. PC1 substrates are adrenocorticotrophic hormone (ACTH), Glucagon-like peptide 1 & 2 (GLP1, GLP2), Growth hormone-releasing hormone (GHRH). And the specific substrates for PC2 are β -endorphin and α -melanocyte-stimulating hormone. Likewise, they can together process the proinsulin, pro-opiomelanocortin (POMC; precursor of adrenocorticotrophic hormone [ACTH] and β -endorphin), melanin-concentrating hormone (MCH), secretogranin II, proenkephalin, prodynorphin, proglucagon, prosomatostatin, chromogranins A and B, and pituitary adenylyl cyclase-activating peptide (PACAP) [113, 117, 118-120].

Furin: is ubiquitously expressed in most tissues. Many of the growth factors such as tumor necrosis factor-beta (TGF β), and receptors such as insulin receptor are substrates of furin. Other substrates include adhesion molecules (α 5 integrin and repulsive guidance molecule BMP co-receptor A (RGMA)), metalloproteinases (MMP14), Proton pump V-ATPase accessory protein Ac45 subunit, Viral glycoproteins (HIV gp160), and Bacterial toxins (anthrax pa83) [115, 121].

PC4: is expressed in reproductive tissues such as testis, oocytes, placenta, germinal cells in the gonads. Insulin-like growth factor-2 (IGF2), pituitary adenylyl cyclase-activating peptide (PACAP), deformed epidermal autoregulatory factor 1 (DEAF-1), proenkephalin, initially translated neurotrophic nerve growth factor (proNGF), proPACAP, hepatocyte growth factor

receptor (HGFR), insulin-like growth factor 1 receptor (IGF-1R), a disintegrin- and metalloproteinase (ADAM) family including ADAM-1, ADAM-2, ADAM-3, and ADAM-5 are known substrates of PC4 [113].

PC5: is expressed in many different tissues. During the alternative splicing, two isoforms of mRNA will produce two different proteins. The PC5A is a soluble protein and PC5B is a type I membrane-bound protein. There are various substrates for PC5 which are not only specific to PC5 and can be also cleaved by PACE4, furin, or PC7. The only specific substrate of PC5 is Growth differentiation factor 11 (GDF11). Other substrates are redundantly cleaved by one or more convertase such as α 4 integrin, L1 cell adhesion molecule (L1CAM), protein Tyrosine phosphatase receptor type M (PTPRM), IGF-1R, matrix metalloproteases and ADAM family enzymes [122-125].

PCSK6 or PACE4: is ubiquitously expressed in many tissues. There are different identified substrates for PACE4 such as Nodal, lefty, a disintegrin, and metalloprotease with thrombospondin motif 4 (ADAM-TS4) and HIV-1-Vpr [126].

PCSK7: is ubiquitously expressed in many tissues and is highly abundant in colon, gut, neurons, and microglia. The only known specific substrate for the PC7 is human transferrin receptor-1 resulting in a prominent role of human PC7 in iron metabolism. Other substrates of PC7 can also be cleaved by Furin and include pro-epidermal growth factor, brain-derived neurotrophic factor (BDNF) and cancer susceptibility candidate 4 (CASC4) [127].

SKI-1/SIP: is ubiquitously expressed in many tissues. Many different transcription factors have been reported as a substrate for the SKI-1 such as sterol regulatory element-binding proteins (SREBPs), cyclic AMP-responsive element-binding proteins (CREBPs). In addition to these

transcription factors, SKI-1 also can cleave the ER-stress response factor ATF6 and CREB-like transcription factors Lumen, cAMP response element-binding protein (CREB4), and α/β -subunit precursor of the N-acetyl galactosamine 1 (GlcNAc-1)-phosphotransferase [113].

PCSK9: is expressed in the liver, kidney, small intestine, and brain cerebellum. The only substrate of PCSK9 is itself as described earlier. In a non-enzymatic fashion, PCSK9 binds to low-density lipoprotein receptor (LDLR), VLDLR and ApoER2 and leads to their lysosomal degradation [128, 129].

1.9. Proprotein convertase subtilisin/kexin type 7 (PCSK7), its structure, biosynthesis, and physiological importance

The proprotein convertase 7 (PC7) is ubiquitously expressed and encodes a type-I membrane-bound protease synthesized in the endoplasmic reticulum (ER), as a ~102-kDa proPC7 zymogen which then undergoes an autocatalytic cleavage to generate an inactive ~92-kDa mature PC7. The pro-domain remains associated with it non-covalently until the whole complex translocates to the Golgi and cell surface where PC7 can be activated in early endosomal-like organelles. The PCK7 gene is located in chromosome 9 in mice and chromosome 11 in human. So far, the only specific substrate identified for PC7 is human transferrin receptor 1 (TfR1). This protein is shed by PC7 and the soluble form will be released into the extracellular space. In previous studies, PC7 knock-out mice were viable and healthy and showed less anxiety (Figure 9) [115, 130-133].

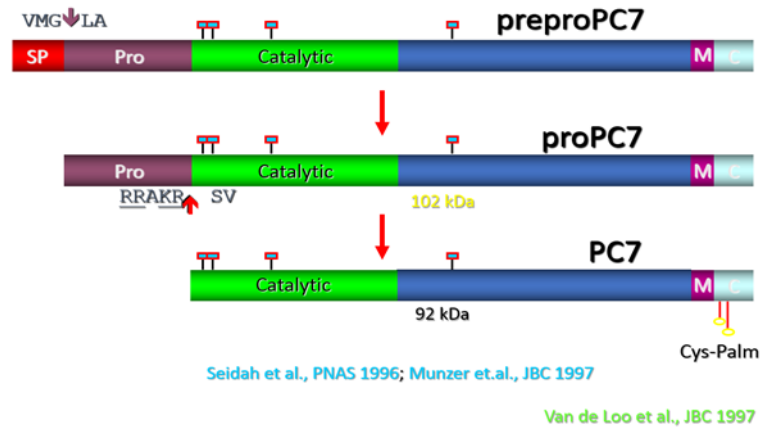


Figure 9: Zymogene processing of Pro-PC7 to PC7 [115].

1.9.1. PC7 association with NAFLD

Various *in vivo* and *in vitro* investigations in recent years, provided evidence indicating a role of PC7 in TG regulation and NAFLD. A recent meta-analysis of genome-wide association revealed the association of the gain-of-function (GOF) non-coding variant (SNP rs236918) in intron 9 of the PC7 gene (*PCSK7*; minor C allele) in elevating the levels of shed sTfR1 in human plasma. Likewise, this polymorphism was reported to cause increased insulin resistance based on a study on obese people with a high carbohydrate diet for 6 months [134]. Previous data from our lab showed that this SNP is significantly associated with 3.5% higher plasma triglyceride (TG) levels ($p=4.6 \times 10^{-119}$) [133].

On the other hand, a whole-exome sequencing analysis among African Americans revealed the significant association of a loss of function single-nucleotide polymorphism (SNP) of PC7 (p. Arg504His; SNP rs142953140) with almost 30% reduction in TG levels and almost 40% enhanced high-density lipoproteins (HDL). [135] similarly, another study confirmed that mice overexpressing human PC7 in the liver showed ~45% higher plasma TG compared to wild-type (WT) mice. Interestingly, previous studies in our lab indicated that this PC7-R504H variant does

not affect the enzymatic activity of PC7 on its substrates such as human transferrin 1 and sortilin, or apolipoprotein F suggesting a novel non-enzymatic function for PC7.

Based on another investigation in our lab, the VLDL-TG secretion and TG production were measured in wild-type (WT) and *Pcsk7^{-/-}* mice. Their results suggest that only under normal diet (ND) there is a significant reduction in TG and ApoB levels (inside and outside the cells) meaning that lack of PC7 results in less TG inside the cells, probably due to trigger of FA oxidation because of TG accumulation in the ER and subsequently less secreted TG outside due to lower ApoB levels. A very new ongoing investigation in our lab confirmed this hypothesis and showed that the PC7 can acts as a chaperone for the proper folding and secretion of ApoB. Therefore, lower PC7 results in the degradation of ApoB leading to ER stress (due to accumulation of TG in the ER) and higher autophagy and beta-oxidation, and finally lower TG (in LD) [136].

1.10. Transmembrane 6 superfamily 2 protein (TM6SF2), its structure, biological function, and association with NAFLD

As we mentioned earlier, *TM6SF2* is one of the most important genes involved in NAFLD and *TM6SF2* variants have 7% allelic frequency among patients with NAFLD. The *TM6SF2* gene is located on chromosome 19p13.11 with 10 exons, encodes a protein of 377 amino acids with two different isoforms which are different at the C-terminal. TM6SF2 consists of 7-10 predicted transmembrane domains with a molecular weight of 39.5-kDa. TM6SF2 is localized in ER and Golgi and it is mostly expressed in the liver, small intestine, and kidney [137,138, 139]. Recently, exome-wide association studies revealed a missense variant (rs58542926) in *TM6SF2*, in which adenine is replaced by guanine in coding nucleotide 499 resulting in replaces of glutamate with

lysine at residue 167 (c.499A_G; p. Glu167Lys). This study showed the significant association of this variant with NAFLD and results in the development of steatosis in carriers. Also, this variant leads to instability of the TM6SF2 protein with a reduced half-life and is thus considered as a LOF variant [140-145].

So far, the function of TM6SF2 protein has been unknown until very recent investigations which demonstrate the role of TM6SF2 in VLDL lipidation. According to a study in 2016, the inactivation of the *TM6SF2* gene in mice results in a significant accumulation of TG in hepatocytes and enterocytes compared to WT mice. Therefore, they indicated that TM6SF2's role is to lipidate apoB containing lipoproteins without affecting the secretion of this particle from the liver. Their proposed model for the TM6SF2 function explains that TM6SF2 transport neutral lipids from lipid droplets across the ER membrane through one of the three following mechanisms: transferring to MTP, transferring to neutral LD, or transferring directly to the VLDL particle (Figure 10) [146].

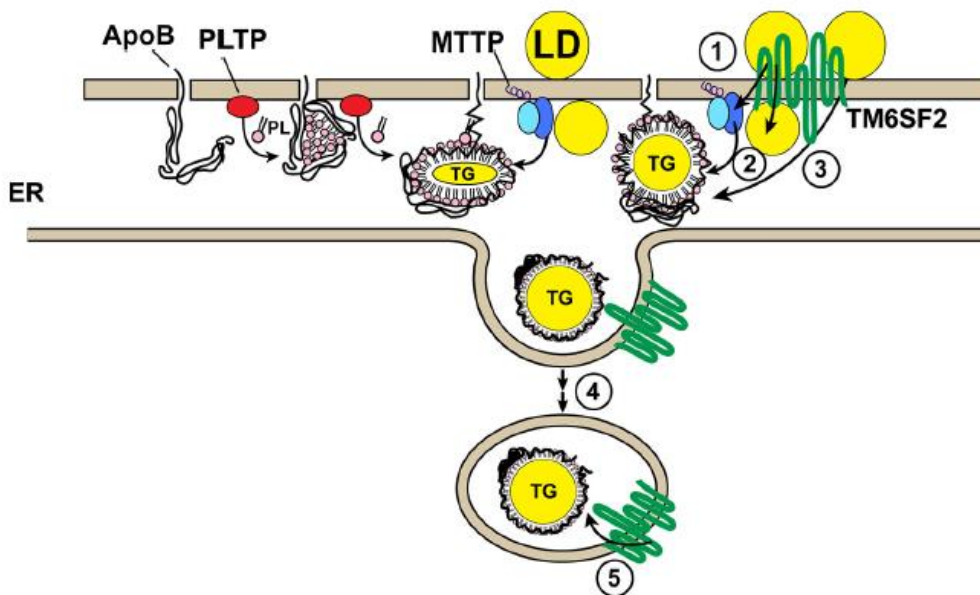


Figure 10. Schematic of the Proposed model for the TM6SF2 role in lipidation of VLDL particles [146].

Another study [147] confirmed the prominent role of TM6SF2 protein in the secretion of VLDL particles. According to their data, hepatic overexpression of *Tm6sf2* in mice using adeno-associated virus (AAV)-mediated gene delivery, resulted in accumulation of apoB in the endoplasmic reticulum (ER) and subsequently a significant decrease in apoB secretion. As we will see later in our results, overexpression of *TM6SF2* also results in enhanced degradation of PC7, which may also contribute to the reduced apoB secretion observed.

Interestingly, a recent investigation [148], revealed that TM6SF2 and ApoB are interacting proteins in a complex. They indicated that the two proteins stabilize each other in the complex. Also, they showed that in *Tm6sf2* knockdown mice, there are reduced apoB protein levels which further resulted in lower secretion of lipids in the circulation and accumulated TGs in the liver. They indicated that this could be an explanation for the elevated TG seen in the patients with *TM6SF2 E167K* mutation. Because the E167K mutation destabilizes the TM6SF2 protein and results in reduced protein levels of TM6SF2. Based on these results, lower protein levels of TM6SF2 lead to destabilization of ApoB and subsequently less secretion of the VLDL particles and accumulation of lipids in the ER.

Hypothesis and Objectives.

Based on the finding of the previous investigations and recent studies in our lab, we hypothesize that silencing of *PCSK7* can reduce the TG accumulation in liver cells and represents a potential target for the treatment of NAFLD.

My major work in this project is:

- 1) finding a promising way for silencing of *PCSK7* to achieve an effective treatment for NAFLD. Pursuing this aim, we have decided to use antisense oligonucleotide (ASO) technology.

Our second hypothesis is that the TM6SF2 and PC7 may interact with each other since they both are localized in the ER and Golgi, both interact with ApoB protein affecting its stability, and result in TG accumulation in the ER. So far, there not any study on the relationship between these two proteins.

Therefore, my second aim in this work is:

- 2) To define the relationship between the proteins PC7 and TM6SF2 using *in vitro* assays.

Chapter 2:

Material & methods.

2.1. Reagents and Plasmids

The human complementary deoxyribonucleic acids (cDNAs) encoding TM6SF2-WT, TM6SF2-E167K, and TM6SF2-S165E were cloned in pcDNA3.1 vector with a flag tag on their C-termini. The human PC7-WT and PC7D188G were cloned in PIRE5 vector with a V5 tag on their C-termini. All the mutants were generated using site-directed mutagenesis and the integrity of their sequences was verified using whole DNA sequencing.

2.2. The design of ASOs

We designed 8 ASOs against the human *PCSK7* gene, 8 ASOs against the Mouse *Pcsk7* gene, and two scrambled ASOs using the primer quest tool from Integrated DNA Technologies (IDT) (<https://www.idtdna.com>). The ASOs were 20-mer oligonucleotides containing phosphorothioate and 2'-O-methoxyethyl groups between each nucleotide and were provided by Integrated DNA Technologies (IDT). The sequences of all the ASOs are listed as follows:

Table 4: The human and mouse sequences of antisense oligonucleotides (ASOs)

ASO-ID (Human)	Sequence	Exon
hs_PCSK7_ASO1	/56-FAM/mG*mA*mC*mG*mU*A*G*G*A*T*G*C*T*A*A*mG*mU*mA*mA*mG	Exon12
hs_PCSK7_ASO2	/56-FAM/mA*mU*mG*mG*mA*G*T*T*G*G*C*G*T*A*G*mC*mC*mA*mU*mC	Exon8
hs_PCSK7_ASO3	/56-FAM/mG*mA*mU*mC*mU*G*A*T*A*G*T*G*C*T*T*mG*mU*mU*mG*mA	Exon6
hs_PCSK7_ASO4	/56-FAM/mC*mA*mG*mC*mA*T*T*A*A*G*G*C*T*A*T*mC*mA*mU*mG*mC	Exon10

hs_PCSK7_ASO5	/56-FAM/mC*mA*mC*mU*mU*T*C*A*C*T*G*T*G*A*G*mU*mA*mG*mU*mG	Exon2
hs_PCSK7_ASO6	/56-FAM/mC*mA*mC*mA*mU*T*C*T*T*C*T*G*C*A*T*mA*mG*mA*mA*mA	Exon9
hs_PCSK7_ASO7	/56-FAM/mC*mC*mC*mC*mC*A*G*C*A*T*C*G*C*A*C*mA*mG*mU*mG*mG	Exon14
hs_PCSK7_ASO8	/56-FAM/mU*mC*mC*mA*mA*G*T*G*T*G*G*C*A*C*T*mU*mU*mC*mU*mG	Exon3
ASO-ID (Mouse)	Sequence	Exon
mm_Pcsk7_ASO1	/56-FAM/mA*mC*mA*mG*mU*G*G*C*A*T*T*G*A*T*T*mC*mU*mA*mG*mU	Exon17
mm_Pcsk7_ASO2	/56-FAM/mC*mU*mC*mC*mA*T*A*C*T*G*T*C*A*G*T*mA*mA*mG*mU*mG	Exon6
mm_Pcsk7_ASO3	/56-FAM/mC*mU*mG*mA*mU*A*A*C*C*A*G*T*C*T*G*mU*mA*mG*mA*mC	Exon14
mm_Pcsk7_ASO4	/56-FAM/mA*mU*mC*mA*mU*A*G*T*T*G*C*A*G*T*T*mG*mU*mC*mA*mU	Exon8
mm_Pcsk7_ASO5	/56-FAM/mG*mA*mC*mA*mU*A*G*G*A*G*G*C*T*A*A*mG*mU*mA*mA*mG	Exon12
mm_Pcsk7_ASO6	/56-FAM/mU*mG*mA*mG*mU*G*T*C*G*A*C*T*G*G*mA*mA*mC*mA*mC	Exon2
mm_Pcsk7_ASO7	/56-FAM/mG*mA*mU*mG*mU*C*T*C*T*T*C*C*T*G*G*mG*mC*mU*mC*mC	Exon4
mm_Pcsk7_ASO8	/56-FAM/mG*mA*mU*mC*mU*G*G*G*T*C*A*T*T*A*G*mA*mG*mU*mU*mG	Exon5
ASO-ID (Scrambles)	Sequence	
Neg_CTRL_B	/56-FAM/mG*mC*mG*mU*mA*T*T*A*T*A*G*C*C*G*A*mU*mU*mA*mA*mC	
IDT_StdNeg_CTRL	/56-FAM/mC*mG*mA*mC*mU*A*T*A*C*G*C*G*C*A*A*mU*mA*mU*mG*mG	

2.3. Cell culture and cDNA transfections

Two different human cell lines including IHH (immortalized human hepatocytes), HepG2 (human hepatocellular carcinoma), and one Mouse cell line called FL83B (Mouse hepatocytes) were grown in Dulbecco's Modified Eagle Medium (DMEM) media with 10% fetal bovine serum (FBS), Eagle's Minimum Essential Medium (EMEM) media with 10% FBS, Kaighn's Modification of Ham's F-12 (F12K) media with 10% FBS (Invitrogen), respectively. The cells were maintained at 37°C under 5% CO₂. The transfection of TM6SF2, its mutants, PC7, and its mutant for the western blot analysis was done using FuGENE®HD (Promega) in HepG2 cells, JETPEI (PolyPlus) in IHH cells. 48 hours post-transfection the cell lysate was collected. The ASOs and siRNAs were transfected by Dharmafect 4 reagent (dharmacon) for further analysis.

2.4. Western blotting (WB)

Proteins were extracted from cultured cells using 50 mM Tris-HCl pH (power of hydrogen) 8, 150 mM NaCl, 0.1% sodium dodecyl sulfate (SDS), 1% NP-40 and 0.25% Na deoxycholate (RIPA 1x) buffer with 4% protease inhibitor cocktail with ethylenediaminetetraacetic acid (EDTA) (Roche). Bradford assay was performed for the protein concentrations. Proteins were resolved on 6.5% and 12% tris-glycine sodium dodecyl sulfate-polyacrylamide gel electrophoresis (SDS-PAGE) and blotted onto polyvinylidene fluoride or polyvinylidene difluoride (PVDF) membranes. Then, membranes were then incubated with the related primary and secondary antibodies following by their analysis and quantification by the ChemiDoc imaging system (Biorad).

2.5. Quantitative real-time PCR

Total RNA was extracted from cultured cells using Trizol (Sigma). The RNA was pooled for cDNA synthesis using oligo dT, random hexamer, and reverse transcriptase. Then the same amount of cDNAs were used for the analysis of gene expression using quantitative real-time polymerase chain reaction (PCR).

2.6. Cell viability assay (MTS)

For the viability assay, we used the CellTiter 96® Aqueous One Solution Cell Proliferation Assay (MTS) (Promega). The IHH and FL83B cells were plated on a 96 well plate following by transfection with ASOs. Around 48 hours post-transfection, 20µl of CellTiter 96® Aqueous One Solution Reagent was added into each well for a final volume of 120µl (including culture medium). Then the plate was incubated at 37°C for 3 hours in a humidified, 5% carbon dioxide (CO₂) atmosphere. the viability of the cells was measured by a 96-plate reader machine which measure records the absorbance at 490nm wavelength.

2.7. Flow Cytometry (FACS)

The cultured cells were trypsinized and washed with PBS. the suspended cells were diluted in polystyrene tubes containing 1%FBS and immediately introduced into the flow cytometer. For each sample, 10000 events were used for collecting the data. After recording the forward scatter (FSC), side scatter (SSC) and green fluorescence (FL1), FSC and SSC data were used to identify viable cells. We set the gates to exclude cellular debris. The derived data were analyzed as described by the software.

2.8. Oil Red O staining

The IHH and FL83B Cells were grown on glass coverslips (100,000 cells/well) covered with Poly L lysine. After appropriate time points (72 hours and 120 hours post-transfection for the FL83B and IHH cells, respectively), the cells were fixed with 4% paraformaldehyde in PBS at room temperature for 30 min. After PBS and 60% isopropyl alcohol wash, cells were stained with Oil Red O solution for 7 minutes. Cells were washed with distilled water and 60% isopropyl alcohol followed by staining with hematoxylin for 30 seconds. We did the final washes with distilled water and prepared the coverslips on slides with mounting media (without desorption atmospheric pressure photoionization (DAPPI)) for taking the images. The average area of Oil Red O-stained LDs and the number of red dots were normalized by the number of cells.

Chapter 3:

Results.

3.1 Design of ASOs to inhibit PC7 in human and mouse.

To inhibit the *PCSK7* gene, we have designed 8 ASOs against human PC7 and 8 ASOs against mouse PC7. These ASOs were designed on different exons along the *PCSK7* gene. We aimed to identify the ASOs that will give the best inhibition results (Figure 11). Also, we designed two control ASOs as scrambles called NEG and IDT. These two ASOs do not target anything on the human and mouse genome.

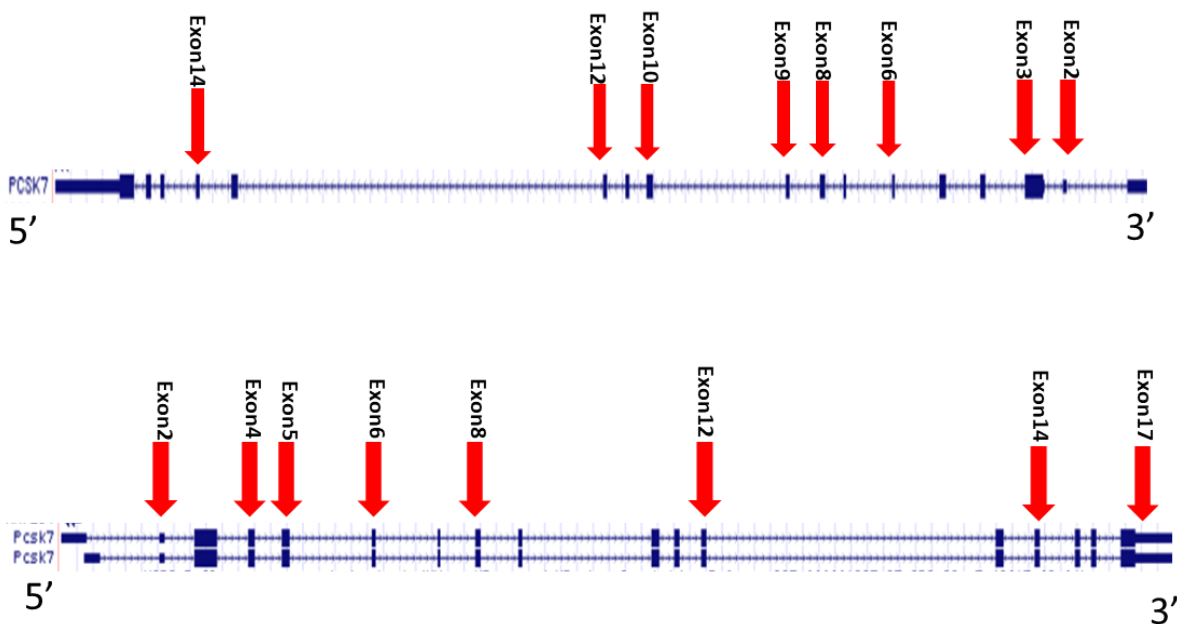


Figure 11. Schematic of designed ASOs on different exons on PCSK7 gene (human and mouse).
1) human PC7 gene. 2) mouse PCSK7 gene.

3.2. Fluorescence-activated single-cell sorting (FACS) results showed high transfection efficiency of ASOs.

Before studying the knock-down efficiency of each of the 16 Antisense Oligonucleotides (ASOs) designed for humans and mouse, we needed to check the transfection efficiency of all of them. Transfection efficiency is a very crucial step for studying gene targeting since it shows us how accurate are the results depending on the number of cells that received the ASOs. In this study, we expected quite a high transfection efficiency (more 70%) for the human and mouse ASOs. Because they are small (20 nts) single-stranded DNAs or RNAs and much smaller compared to plasmids. Note that other parameters can affect the transfection efficiency, including the lipid-based reagents used for delivery of ASOs into the cells and the cell type.

Here, we measured the transfection efficiency of the ASOs using Fluorescence-activated single-cell sorting (FACS). In this experiment, we had one control in which cells were not transfected. Also, due to the influence of lipid-based transfection reagents on the natural fluorescence of cells, we had another control in which cells were transfected with a scramble ASO that does not target anything on the human and mouse genome, and one control in which cells were transfected with transfection reagent only.

One million cells were transfected for each condition. All the ASOs were synthesized with a fluorescent probe (FAM) as reporter. 24 hours after transfection, cells were suspended in PBS and analyzed using flow cytometry to determine the transfection efficiency and cell viability. The FACS results of the transfection of ASOs (25 nM for each well of a 12-well plate) in human hepatocytes (IHH) using Dharmafect reagent showed quite a high transfection efficiency with an average of 86.4% for the 8 ASOs. Also, the viability of these cells was very high and around 94.9% on average. (supplemental image 1)

We did the same experiments with the same reagents and number of cells and control for the mouse ASO in mouse hepatocytes (FL83B cell line). The results from FACS showed, an average of 46.7%

transfection efficiency for the mouse ASOs and an average of 98.1% cell viability. Since the transfection efficiency was not satisfying (although the cell viability was still quite high) we performed cell sorting to select only those cells containing the ASOs. Therefore, the following results for mASOs are after cell sorting. (supplemental image 2) (Figure 12)

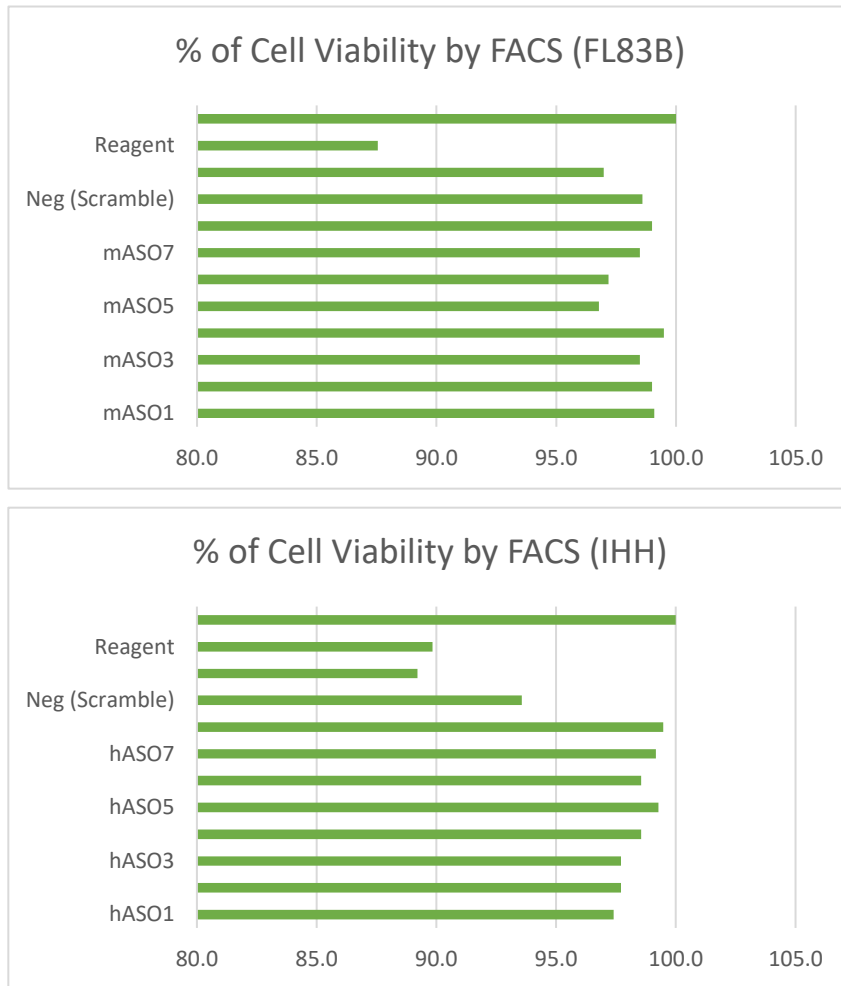


Figure 12. Cell Viability results by FACS after 24 hours post-transfection of human ASOs and mASOs in IHH and FL83B cells, respectively. (number of repeats: 1)

For selecting the best cell line for this *in vitro* study, we have checked the mRNA levels of PC7 in four different cell lines including, IHH, HepG2, HuH7 (human liver cell line), and HK293

(human embryonic kidney 293) (Figure 13). As you can see the IHH and HuH7 have the higher expression of PC7, and both are appropriate for this experiment. But we have selected IHH cells rather than HuH7 (although PC7 is expressed more in HuH7) because the IHH cells are immortalized human hepatocytes that are more similar to human primary hepatocytes.

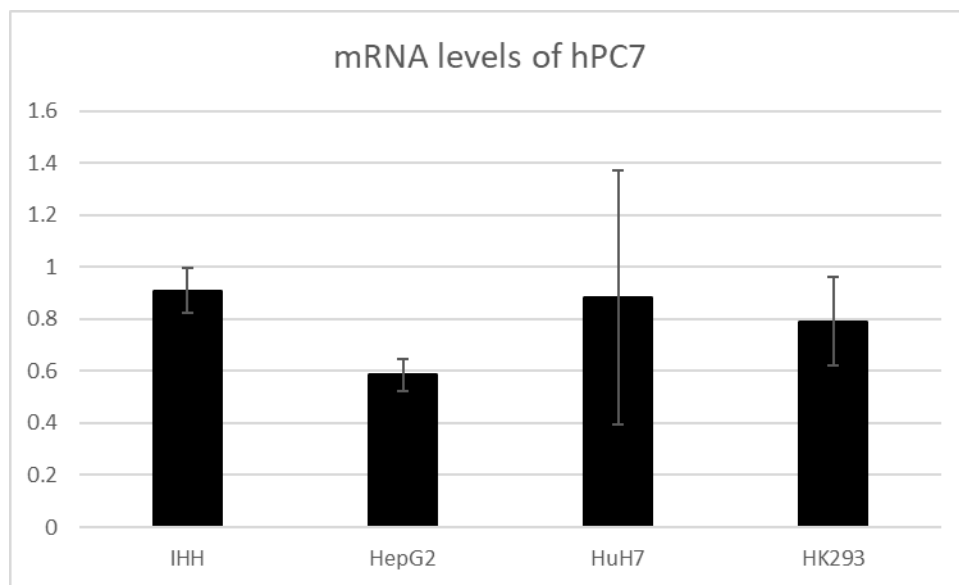


Figure 13: mRNA levels of human PC7 in four different cell lines by qPCR (number of repeats:2). Error bars are SD.

3.3 Cell viability assay (MTS) showed a high percentage of cell viability after treatment with ASOs in both human and mouse cell lines.

Cell viability assay was performed using MTS for the quantification of viable cells of IHH and FL83B after transfecting with human and mouse ASOs, respectively. As illustrated in (Figure 14), the results showed quite high viability of IHH and FL83B cells 48 hours post-transfection. This confirms the results from FACS for the viable cells and indicates that the ASOs do not cause cell mortality and are not toxic to the cells. Here, because of the possible toxicity of the transfection reagents for the cells, we tested a control consisting of the transfection reagent only, and all the results were normalized to that. By doing that, we can reach an accurate percentage of toxicity

caused by ASOs. The results are related to two experiments where each condition was repeated 5 times.

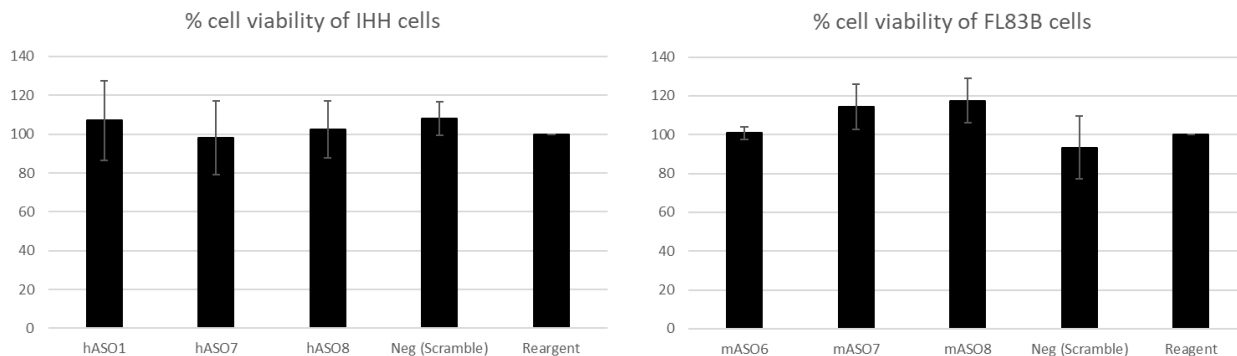


Figure 14. Cell viability measured using MTS assay. Viability was measured after 48 hours post-transfection of cells in a 96-well plate. with human and mouse ASOs. Analyzing was performed by comparing each condition with the reagent-only control. Both cell lines (number of repeats:2). Error bars are SD.

3.4. Human ASOs against the *PCSK7* gene, showed a great reduction of PC7 protein levels and mRNA levels after 72 hours.

We needed to check to see which one of the 8 ASOs designed for human works best. To do that, we did a time-course experiment to select the best time point for collecting our cells and checking the results. We experimented after 48 hours, 72 hours, and 96 hours (the results are not provided here). At all the time points, we could see a significant reduction in the protein and mRNA levels of PC7. Interestingly, after 72 hours we could reach the best results. Although, after 96 hours post-transfection with ASOs we still had a significant reduction with most of the 8 ASOs, it was not as significant as 72 hours post-transfection. However, it could be because of the half-life of the ASOs, or cellular multiplication during the assay, which results in dilution of ASOs.

Here, we can see the results of ASO transfection in IHH in (Figure 15) after 72 hours. As it can be seen, we reached a high inhibition of PC7 expression in all the conditions. However, it seems that

we had the best results with ASOs number 1 and 7 targeting exon 12 and 14 of the human *PCSK7* gene, respectively, both at the protein levels and mRNA levels.

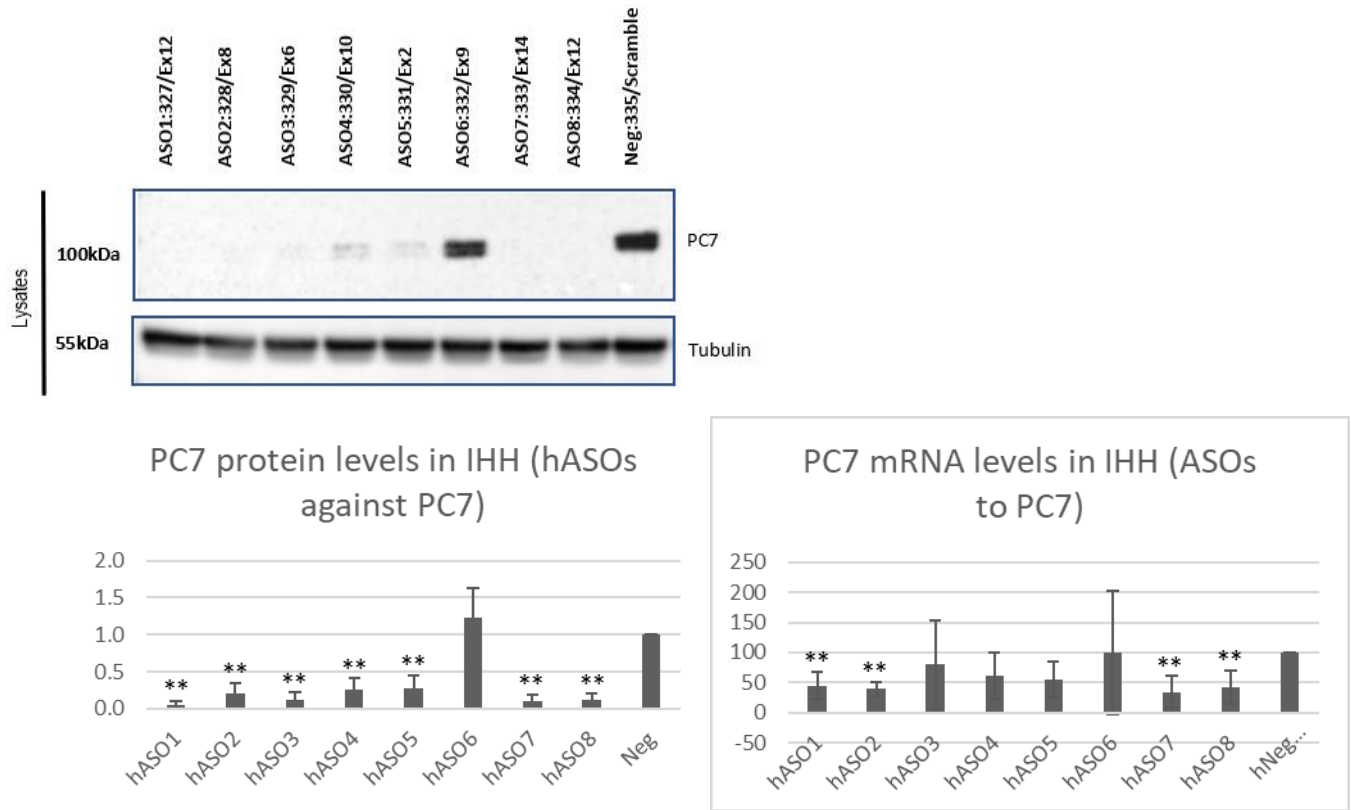


Figure 15. PC7 protein and mRNA levels after transfection with human ASOs. The 8 ASOs were transfection (25nM) in IHH cells (150,000cells/well) by Dharmafect reagent in a 12-well plate and they were collected after 72 hours. PCSK7 (D415G) Rabbit mAb #19346 was used (number of repeats:3). Error bars are SD. ** $p < 0.01$.

3.5. Mouse ASOs against the *Pcsk7* gene, showed a great reduction of PC7 mRNA levels after 72 hours.

We did the same experiment for the mouse ASO in FL83B cells. After 72 hours we could see a significant reduction in the transcripts of PC7 by many of them (the results are not shown here). But ASOs number 6, 7, and 8 showed the best results for PC7 inhibition. Since the transfection efficiency of ASOs in FL83B cells was not adequate, we performed cell sorting using FACS to select for cells that best incorporated the fluorescent ASOs and then measured the mRNA levels of PC7 only on cells transfected by ASOs 6, 7, and 8. (Figure 16). Interestingly, these ASOs resulted in a more than 80 percent decrease in mouse PC7 mRNA.

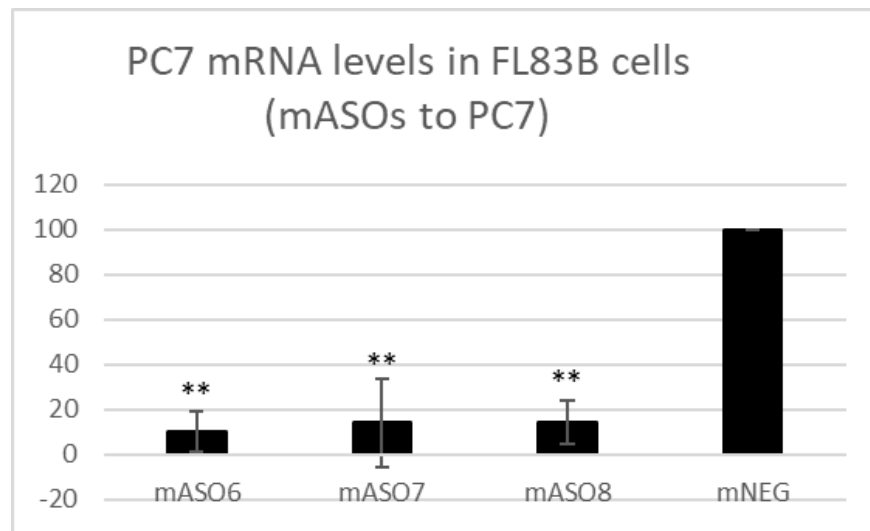


Figure 16. PC7 mRNA levels after transfection with Mouse ASOS number 6, 7, and 8. The ASOs were transfection (25nM) in FL83B cells (150,000cells/well) by Dharmafect reagent in a 12-well plate and they were collected after 72 hours (number of repeats:3). Error bars are SD. ** $p < 0.01$.

Unfortunately, the PCSK7 (D415G) Rabbit mAb #19346 antibody did not work in mouse and so far, there is not available commercial antibody that recognizes mouse PC7 protein for Western blot

(WB) experiments. Therefore, we only have qPCR results for the mRNA of PC7, which revealed a significant reduction in the production of PC7 protein.

3.6. The IHH cells exhibit a highly significant reduction in the number of lipid droplets after 120 hours of treatment with ASO7.

To see if the selected ASOs are functionally active and can provide the expected results, we analyzed the TG content in the IHH cells after transfection with hASO7. Also, we had a scramble Neg control. Accordingly, cells were stained with Oil Red O to stain for neutral lipids (and TG content) After 120 hours, we fixed the cells and analyzed the results (Figure 17). As it is illustrated below, the number of lipid droplets significantly decreased more than 80% after PC7 inhibition by ASO7 compared to Scramble. Likewise, we could see a significant reduction in the size of lipid droplets as well.

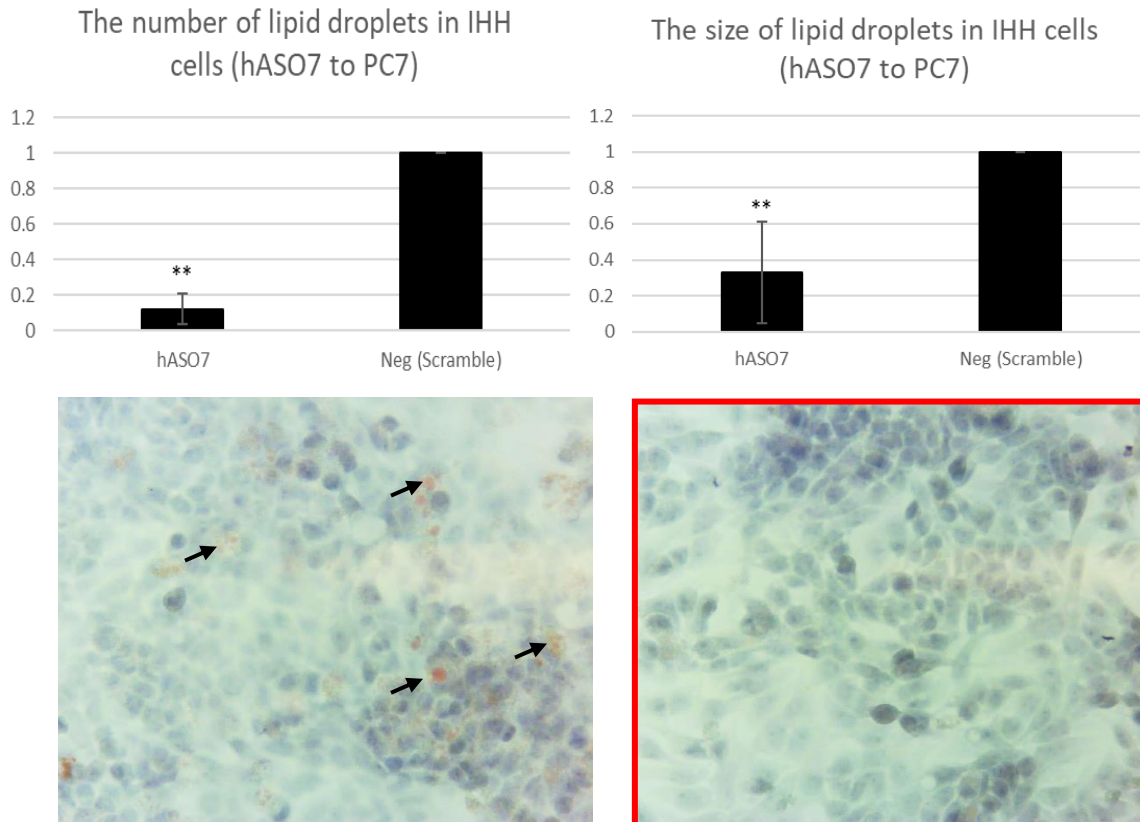


Figure 17. Oil Red O results from hASO7 transfection in IHH cells. The cells were incubated with Oleic acid (0.3mM). After 18 hours we removed the oleic acid and wash with PBS. The ASO7 (25nM) was transfected (12-well plate) by Dharmafect reagent and after 120 hours the cells were fixed and stained with Oil Red O. LDs are shown by arrows. Number of repeats:3. Error bars are SD. * $p < 0.05$; ** $p < 0.01$.

3.7. The FL83B cells exhibit a highly significant reduction in the number of lipid droplets after 72 hours of treatment which ASO7.

We analyzed the TG content in the FL83B cells as well as IHH cells. The cells were transfected with the mouse ASO number 6. Also, we had Neg control as the scramble. In this experiment, we did Oil Red O staining to stain the TG content and after 72 hours, we fixed the cells and analyzed the results (Figure). Our optimization revealed that to the effect of PC7 inhibition we need fewer hours for FL83B cells in comparison to IHH cells. Maybe, it is because of faster fat burning in the mouse. As it is illustrated below, the number of lipid droplets decreased after PC7 inhibition by

ASO7 compared to Scramble, which is highly significant. Although, there was not any significant change in the size of lipid droplets (figure 18).

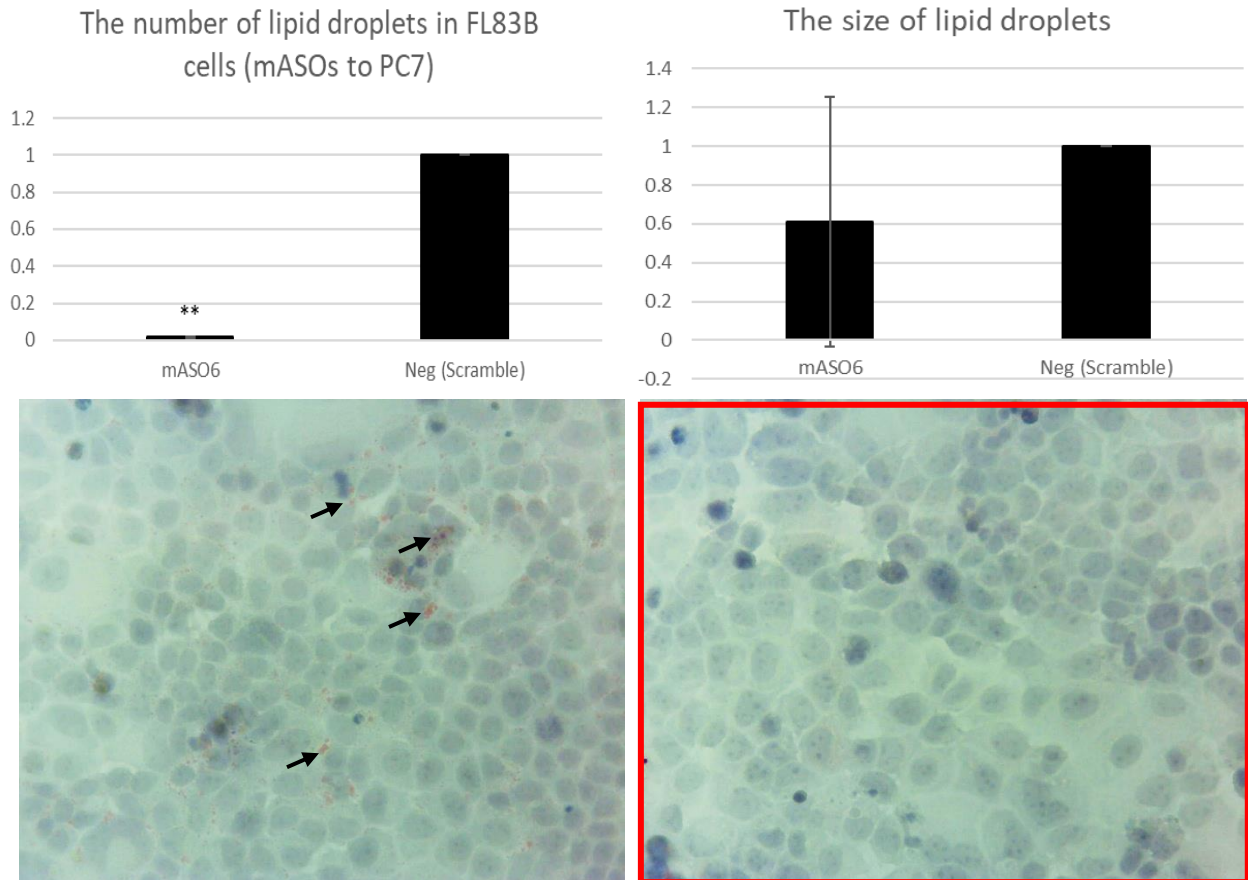


Figure 18. Oil Red O results from mASO7 transfection in FL83B cells. The cells were incubated with Oleic acid (0.3mM). After 18 hours we removed the oleic acid and wash with PBS. The ASO6 (25nM) was transfected (12-well plate) by Dharmafect reagent and after 72 hours the cells were fixed and stained with Oil Red O. The LDs are shown by arrows. Number of repeats:3. Error bars are SD. $**p < 0.01$.

3.8. Denning the relationship between the proteins PC7 and TM6SF2 using *in vitro* assays

For studying the relationship between the TM6SF2 and PC7, hepatic HepG2 cells were co-transfected with cDNAs encoding each C-terminally tagged protein with Flag and V5, respectively. We had three different constructs for the TM6SF2. The first one was the wild-type TM6SF2 protein with full length. Also, we had the cDNA containing the S-X-K167 instead of S-

X-E167, which exactly where the lysine to glutamate mutation occurs in NAFLD patients. On the other hand, the luminal sequence GKYSSEIRP170 is sandwiched between the transmembrane domains 5 and 6 and contains a putative Ser-phosphorylation site for the secretory kinase FAM20C (Golgi associated secretory pathway kinase) that recognizes the S-X-E motif. We hypothesized that the variant S-X-K167 would abrogate phosphorylation at Ser165. Therefore, we synthesized a TM6SF2-S165E construct to mimic such Ser-phosphorylation to probe the role of Ser165-phosphorylation in protein-protein interactions and the stability of TM6SF2 (Figure 19). The SXE/pS is the phosphorylation site for FAM20C (protein kinase)

Human TM6SF2 protein sequence

10	20	30	40	50
MDIPPLAGKI	AALSLSALPV	SYALNHVSAL	SHPLWVALMS	ALILGLLFVA
60	70	80	90	100
VYSLSHGEVS	YDPLYAVFAV	FAFTSVVDLI	IALQEDSYVV	GFMEFYTKEG
110	120	130	140	150
EPYLRTAHGV	FICYWDGTVH	YLLYLAMAGA	ICRRKRYRNF	GLYWLGSFAM
160	170	180	190	200
SILVFLTGNI	LGKYSSEIRP	AFFLTIPYLL	VPCWAGMKVF	SQPRALTRCT
210	220	230	240	250
ANMVQEEQRK	GLLQRPADLA	LVIYLILAGF	FTLFRGLVVL	DCPTDACFVY
260	270	280	290	300
IYQYEPYLRD	PVAYPKVQML	MYMFYVLPFC	GLAAYALTFP	GCSWLPDWAL
310	320	330	340	350
VFAGGIHQAAQ	ESHMGASMHL	RTPFTYRVPE	DTWGCFFVCN	LLYALGPHLL
360	370			
AYRCLQWPAF	FHQPPPSDPL	ALHKKQH		

E167K
S165E

S = Phosphorylation site

Figure 19. Human TM6SF2 protein sequence. The mutation site for the E167K and S165E are shown.

3.9. TM6SF2 enhances the degradation of PC7 but not the ProPCsk7 in both HepG2 and IHH cell lines.

To study the effect of TM6SF2 and PC7 on each other, we co-expressed the PC7 with TM6SF2-WT, TM6SF2-E167K, and TM6SF2-S165E in IHH cells (by JETPEI reagent) and HepG2 cells (Fugene reagent) and after 48 hours did western blot and analyzed the results. Here, we had cDNA of 7B2 protein which does not affect the TM6SF2 and PC7 as a control. As the results are shown

in (Figure 20), The TM6SF2-E167K results in lower levels of protein compared to WT. This agrees with previously reported findings indicating that the E167K variant results in instability of the protein [146]. We propose that this instability could be because of the loss of phosphorylation site for the FAM20C enzyme. Likewise, the expression of TM6SF2-S165E which mimics an enhanced phosphorylation of the protein at Ser165 showed almost 4.7-fold higher protein levels, which supports the notion that phosphorylation of Ser165 stabilizes TM6SF2.

According to these data, the overexpressed complex PCSK7-TM6SF2 is degraded. However, it is very interesting to note that the TM6SF2 enhances only the degradation of PC7 but not the ProPC7.

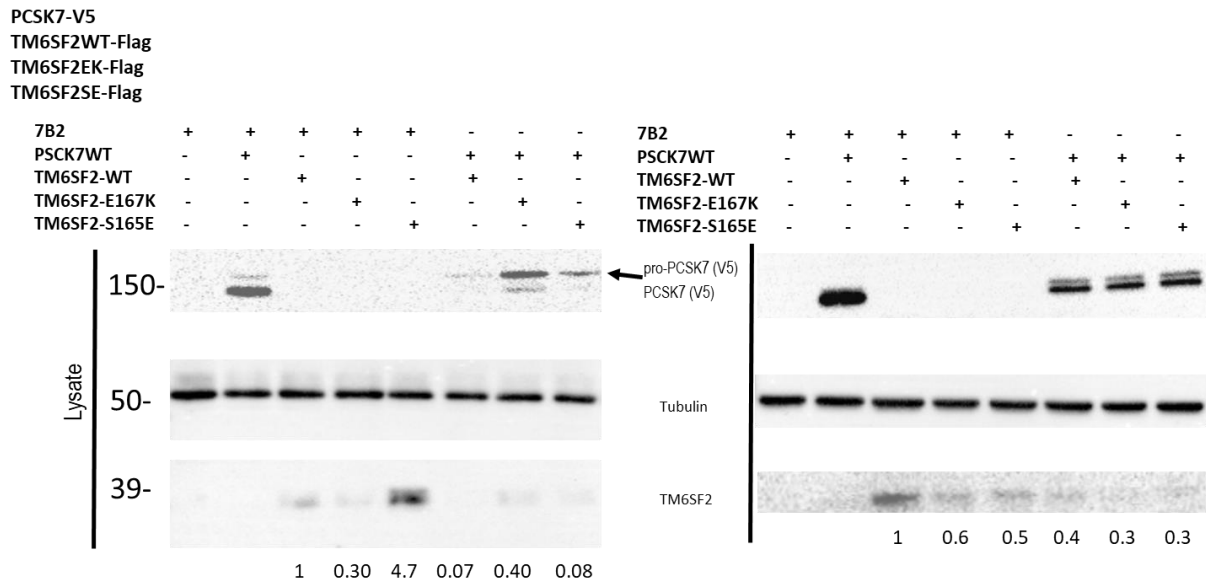


Figure 20. Co-expressing PC7WT cDNA with TM6SF2-WT/TM6SF2-E167K/TM6SF2-S165E. Degradation of the PC7 by TM6SF2 constructs, but not the Pro-PC7. The results are from three repeats.

3.10. TM6SF2 does not affect the levels of ER-localized PC7-D188G (only expresses proPC7)

To investigate whether the TM6SF2 and Pro-PC7 can regulate each other, we generated a PC7-D188G natural variant (immediately after the Asp187 in the catalytic triad) that prevents the zymogen cleavage of proPC7 into PC7 in the ER. As a result, only the Pro-PC7 will be expressed. The results shown in (Figure 21) indicate that TM6SF2 or its mutants do not affect the levels of proPC7.

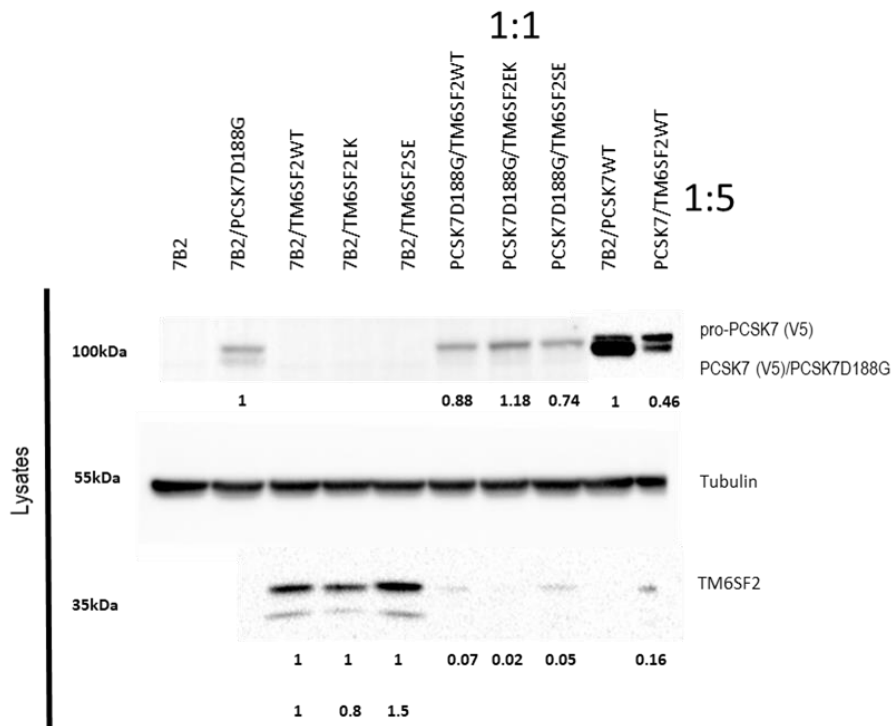


Figure 21. Co-expressing PC7D-188G cDNA with TM6SF2-WT/TM6SF2-E167K/TM6SF2-S165E. There is not any degradation of the Pro-PC7 by TM6SF2 constructs. The results are from three repeats.

3.11. The absence of PC7 does not affect the mRNA and Protein levels of TM6SF2.

To study the functional effect of PC7 on TM6SF2, we measured the mRNA and Protein levels of endogenous TM6SF2 after inhibition of PC7 expression in IHH cells using siRNAs to human PC7. The siRNAs are a set of four different siRNAs (20 nM). We transfected them by Dharmafect and the results were analyzed 72 hours post-transfection. According to our results, in the absence of PC7, there is no significant change in the protein and mRNA levels of TM6SF2 (Figure 22).

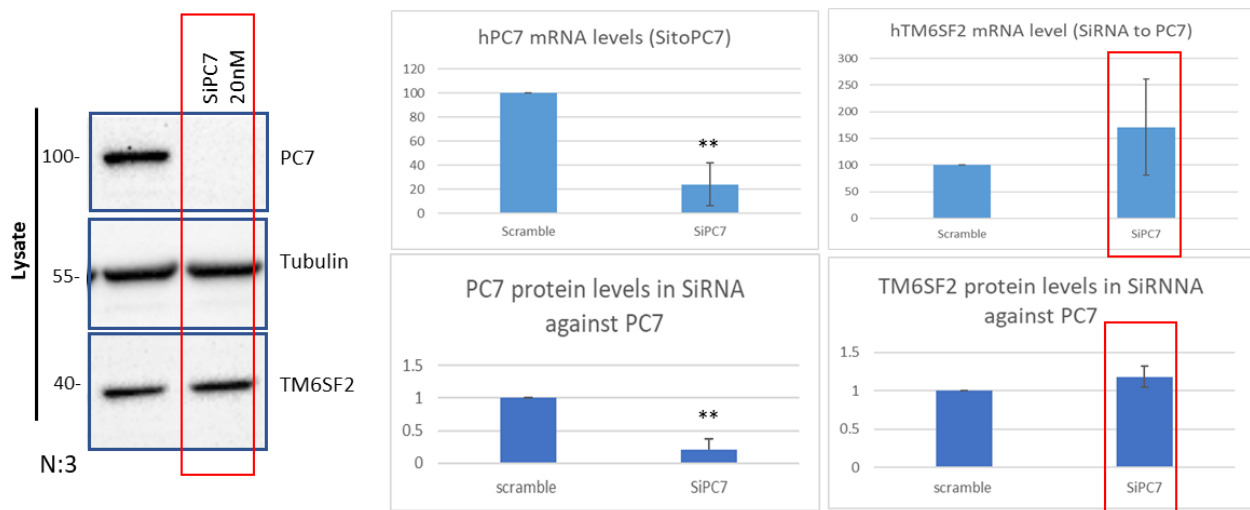


Figure 22. The TM6SF2 mRNA and protein levels 72 hours after PC7 inhibition using siRNAs (20nM) in IHH cells. The results are from three repeats. Error bars are SD. ** $p < 0.01$.

3.12. The protein and mRNA levels of PC7 significantly decreased in the absence of TM6SF2 in IHH cells using siRNAs to TM6SF2.

To see how the *TM6SF2* knockdown will affect the PC7, we used siRNAs to human *TM6SF2* (100nM) in IHH cells using Dharmafect reagent and after 72 hours we check the mRNA and protein levels of PC7 using qPCR and western blot, respectively. Interestingly, as the results are

shown in (Figure 23), there is a significant reduction in both mRNA and protein levels of PC7 after inhibition of TM6SF2. These data suggest that the presence of the TM6SF2 may stabilize the PC7 mRNA and protein.

Although the siRNAs to *TM6SF2* could perfectly reduce the mRNA levels of this gene, the reduction of the TM6SF2 protein level is not adequate, which can be explained because of the longer half-life and turnover of the protein.

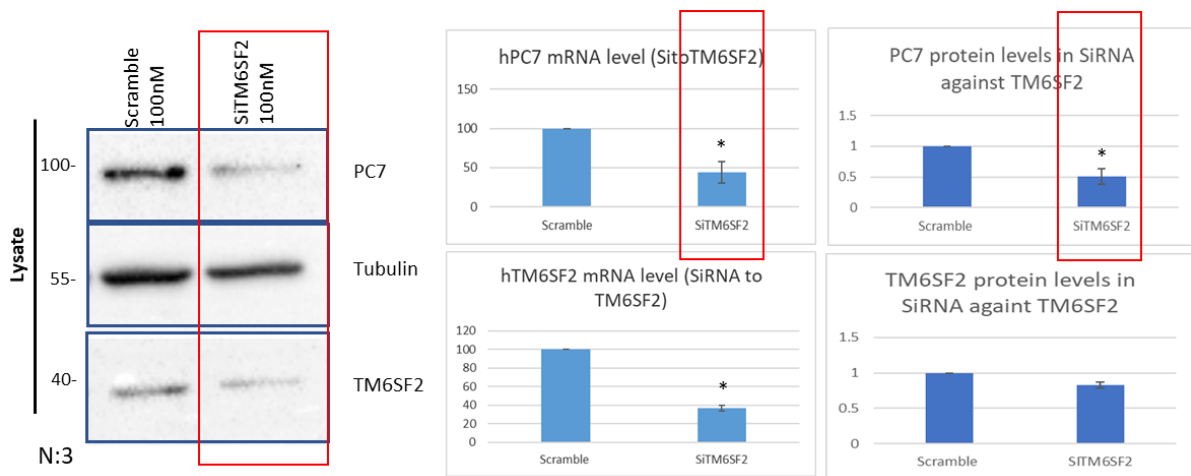


Figure 23. The PC7 mRNA and protein levels 72 hours after TM6SF2 inhibition using siRNAs (100nM) in IHH cells. The results are from three repeats. Error bars are SD. * $p < 0.05$.

Chapter 4:

General discussion and future perspectives.

Non-alcoholic fatty liver disease (NAFLD) is the most preventable liver disease, and it is becoming the major cause of liver-related mortality worldwide. However, there are no approved pharmacotherapies for the treatment of NAFLD. So far, only diet and lifestyle modifications are recommended to patients with early stages of fatty liver disease. The Vitamin E and some other treatments for diabetes such as metformin are recommended but are not very potent. Moreover, liver transplantation, which is an invasive method, is recommended only for those with hepatocarcinoma. Therefore, there is an increasing need for effective and promising treatment for the disease which can prevent the development of steatosis and fibrosis in these patients.

The aim of this project was applying antisense oligonucleotide technology for the inhibition of the proprotein convertase # 7 (PC7) gene (*PCSK7*) as a novel potential therapeutic approach. Based on recent investigations in Dr. Seidah's lab, there are lower apoB protein levels (almost 0%) in both the liver and plasma of the liver specific PC7 KO mice comparing to PC7 WT mice. Therefore, lower PC7 results in the degradation of apoB [136]. Interestingly, another study in 2016 revealed that the absence of ApoB results in an accumulation of TG in the ER, leading to ER stress, which triggers the formation of ER-associated autophagosomes and autophagy ultimately progressing to beta-oxidation of TGs [103]. More recent results *via* co-immunoprecipitation (Co-IP) showed that PC7 binds to ApoB and acts as a chaperone assisting the correct folding of ApoB in the ER, thereby enhancing its secretion in VLDL particles. These results showed that PC7 plays an important role in TG-rich lipoprotein metabolism by regulating apolipoproteins. Accordingly, under normal diet (ND), the livers of *Pcsk7^{-/-}* mice exhibit lower TG levels associated with an

increase of β -oxidation and lower apolipoprotein B (ApoB) levels due to its enhanced degradation in the ER [136]. These findings alongside previous studies on different SNPs on PC7 and their association with NAFLD, confirm that silencing *PCSK7* may represent a potential therapeutic approach for the treatment of NAFLD and steatosis.

During the last few years, the development of ASO therapies for various diseases including spinal muscular atrophy, Huntington's disease, Alzheimer's disease, amyotrophic lateral sclerosis, Parkinson's disease, and more others, increased rapidly. Hence, the focus of the pharmaceutical industry is enhanced on ASO development instead of other similar technologies.

In this project, we designed a total of 17 ASOs: 8 against human PC7 and 8 against mouse PC7 and one control scrambled ASO (NEG). They were efficiently transfected into either IHH cells (Human primary hepatocytes) and FL83B cells (Mouse hepatocytes). These ASOs had some modifications in their structure. For example, 2'-O-methylation protects them against nuclease degradation and immune response. Also, the addition of phosphorothioate (PS), enhances their stability and their binding to serum proteins. This modification enhances their half-lives in circulation and provides more time for them to be entered into the target cells. Our viability tests, using MTS and FACS showed a high percentage of live cells, indicating that the toxicity of these ASOs in cells is low. Transduction of ASOs in IHH cells led to a ~70% reduction in *PCSK7* mRNA levels and almost 90% reduction in its protein levels. Likewise, ASOs in mouse hepatic cells led to a ~80% reduction in *Pcsk7* mRNA levels. Among all the designed ASOs, we found ASO number 7 (hASO7) in humans and number 6 (mASO6) in mouse the most efficient ones. These results indicate that the ASOs were successful *in vitro* for inhibition of *PCSK7* expression.

Functional assays were performed aimed to measure the number and size of lipid droplets (LD) by Oil red O staining. The results showed a highly significant decrease in the number of LD in IHH

cells transfected by hASO7 to PC7 in comparison with those transfected with the NEG ASO. We also could see a significant reduction in the size of LDs. The same results from mASO6 in FL83B (mouse hepatocytes) showed a highly significant decrease in the number of LDs, but not any significant change in the size of lipid droplets. We could see these results using a low sugar medium after 72 hours to 120 hours in FL83B a and IHH cells, respectively. Our results provide strong *in vitro* evidence for the proper function of these ASOs both in the human and mouse. For further examination of these ASOs, they should be tested *in vivo*. These ASOs can be targeted to the liver by the addition of N-acetyl galactosamine (GalNAc) which binds to asialoglycoprotein receptor 1(ASGR1). This step is an ongoing project and currently, three of the ASOs in mice are selected and designed with N-acetyl galactosamine (GalNAc).

In the second part of this project, we have some preliminary results on the PC7 and TM6SF2 relationship. The transmembrane 6 superfamily 2 (TM6SF2) is one of the most important proteins associated with NAFLD. This protein localizes at the membrane of the endoplasmic reticulum (ER) and Golgi. Until recently, the biological function of this protein was unknown. New investigations indicated that TM6SF2 acts as a regulator of liver fat metabolism by modulating triglyceride secretion through VLDLs. Indeed, the data suggests that TM6SF2 promotes the lipidation of VLDL particles by transporting neutral lipids from lipid droplets (LD) to VLDL particles by transferring lipids from neutral LD to MTP and then to the ER lumen, or directly to the nascent VLDL particle [146]. On the other hand, another report showed that TM6SF2 and ApoB proteins stabilize each other by forming a complex in the ER. In NAFLD patients, the associated E167K mutation reduces TM6SF2 levels. Therefore, TM6SF2 does not adequately stabilize ApoB as the WT form, which may result in defective lipidation or secretion of ApoB-containing lipoprotein particles [148]. Conversely, another study indicated that overexpression of

TM6SF2 leads to ApoB-accumulation in the ER, thereby reducing its secretion [147]. These results suggest that maybe TM6SF2 and PC7 interact with each other since both affect the ApoB protein levels and are associated with TG levels in the liver. According to our results, co-expression of TM6SF2 WT, TM6SF2 E167K and TM6SF2 S165E with PC7-WT in IHH and HepG2 cells showed a significant decrease of PC7 levels but not those of its zymogen proPC7, suggesting that TM6SF2 may bind to proPC7, trapping it together with ApoB in the ER. It seems that these results are specific to PC7 but not the other PCs (e.g., Furin or PCSK9, the results of Co-expression of TM6SF2 with other PCs are not shown). Also, the TM6SF2 S165E mimics an enhanced phosphorylation of Ser165 by the secretory kinase FAM20C that recognizes the motif S-X-E. Phosphorylation at Ser165 by FAM20C may result in the stabilization of TM6SF2, since the *TM6SF2 S165E* variant is more stable. In contrast, the *TM6SF2 E167K* variant cannot be phosphorylated at Ser165, likely leading to destabilization of the protein and reduced levels compared to WT.

Knockdown of PC7 using siRNA to PC7 in IHH cells did not lead to any significant change in the TM6SF2 protein and mRNA levels. In contrast, knockdown of TM6SF2 using siRNA to *TM6SF2* in IHH cells leads to a significant reduction in the PC7 protein and mRNA levels suggesting that the TM6SF2 can directly or indirectly affect the function and expression of PC7. These are preliminary results that indicate the TM6SF2 can be considered as a potential regulator or inhibitor for PC7. Since silencing of *TM6SF2* leads to an accumulation of LD in the cytosol, its concomitant effect on lowering PC7 may represent a compensatory protective mechanism in order to enhance β -oxidation and alleviate the toxic effects high levels of LD. Based on these results we hypothesize that TM6SF2 may bind to and/or facilitates the formation of the ApoB-PC7 (and/or proPC7) complex, thereby trapping it in the ER. If validated, the TM6SF2 would be a new regulator for

PC7. In conclusion, our results provide the first evidence of the relationship of the possible direct or indirect interaction of TM6SF2 and PC7, and further investigations are required to validate this concept.

References:

1. Zamecnik, Paul C., and Mary L. Stephenson. "Inhibition of Rous sarcoma virus replication and cell transformation by a specific oligodeoxynucleotide." *Proceedings of the National Academy of Sciences* 75.1 (1978): 280-284.
2. Stephenson, Mary L., and Paul C. Zamecnik. "Inhibition of Rous sarcoma viral RNA translation by a specific oligodeoxyribonucleotide." *Proceedings of the National Academy of Sciences* 75.1 (1978): 285-288.
3. Kilanowska, Anna, and Sylwia Studzińska. "In vivo and in vitro studies of antisense oligonucleotides—a review." *RSC Advances* 10.57 (2020): 34501-34516.
4. Mercuri, Eugenio, et al. "Nusinersen versus sham control in later-onset spinal muscular atrophy." *New England Journal of Medicine* 378.7 (2018): 625-635.
5. Cirak, Sebahattin, et al. "Exon skipping and dystrophin restoration in patients with Duchenne muscular dystrophy after systemic phosphorodiamidate morpholino oligomer treatment: an open-label, phase 2, dose-escalation study." *The Lancet* 378.9791 (2011): 595-605.
6. Scoles, Daniel R., Eric V. Minikel, and Stefan M. Pulst. "Antisense oligonucleotides: A primer." *Neurology Genetics* 5.2 (2019).
7. Lonardo, Amedeo, et al. "AISF position paper on nonalcoholic fatty liver disease (NAFLD): Updates and future directions." *Digestive and Liver Disease* 49.5 (2017): 471-483.
8. Lonardo, Amedeo, et al. "Hypertension, diabetes, atherosclerosis and NASH: cause or consequence?." *Journal of hepatology* 68.2 (2018): 335-352.
9. Kleiner, David E., and Hala R. Makhlof. "Histology of nonalcoholic fatty liver disease and nonalcoholic steatohepatitis in adults and children." *Clinics in liver disease* 20.2 (2016): 293-312.
10. Sørensen, Henrik Toft, et al. "Risk of cancer in patients hospitalized with fatty liver: a Danish cohort study." *Journal of clinical gastroenterology* 36.4 (2003): 356-359.
11. Yasui, Kohichiroh, et al. "Characteristics of patients with nonalcoholic steatohepatitis who develop hepatocellular carcinoma." *Clinical Gastroenterology and Hepatology* 9.5 (2011): 428-433.

12. Friedman, Scott L., et al. "Mechanisms of NAFLD development and therapeutic strategies." *Nature medicine* 24.7 (2018): 908-922.
13. Fazel, Yousef, et al. "Epidemiology and natural history of non-alcoholic fatty liver disease." *Metabolism* 65.8 (2016): 1017-1025.
14. Sayiner, Mehmet, et al. "Epidemiology of nonalcoholic fatty liver disease and nonalcoholic steatohepatitis in the United States and the rest of the world." *Clinics in liver disease* 20.2 (2016): 205-214.
15. Lonardo, Amedeo, et al. "AISF position paper on nonalcoholic fatty liver disease (NAFLD): Updates and future directions." *Digestive and Liver Disease* 49.5 (2017): 471-483.
16. Cobbina, Enoch, and Fatemeh Akhlaghi. "Non-alcoholic fatty liver disease (NAFLD)– pathogenesis, classification, and effect on drug metabolizing enzymes and transporters." *Drug metabolism reviews* 49.2 (2017): 197-211.
17. Wainwright, Patrick, and Christopher D. Byrne. "Bidirectional relationships and disconnects between NAFLD and features of the metabolic syndrome." *International journal of molecular sciences* 17.3 (2016): 367.
18. Ahmed, Monjur. "Non-alcoholic fatty liver disease in 2015." *World journal of hepatology* 7.11 (2015): 1450.
19. Lonardo, Amedeo, et al. "NAFLD in some common endocrine diseases: prevalence, pathophysiology, and principles of diagnosis and management." *International journal of molecular sciences* 20.11 (2019): 2841.
20. Buzzetti, Elena, Massimo Pinzani, and Emmanuel A. Tsochatzis. "The multiple-hit pathogenesis of non-alcoholic fatty liver disease (NAFLD)." *Metabolism* 65.8 (2016): 1038-1048.
21. Lonardo, Amedeo, et al. "Hypertension, diabetes, atherosclerosis and NASH: cause or consequence?." *Journal of hepatology* 68.2 (2018): 335-352.
22. Ballestri, Stefano, et al. "Nonalcoholic fatty liver disease is associated with an almost twofold increased risk of incident type 2 diabetes and metabolic syndrome. Evidence from a systematic review and meta-analysis." *Journal of gastroenterology and hepatology* 31.5 (2016): 936-944.

23. Lin, Shih-Yi, et al. "Risk of acute coronary syndrome and peripheral arterial disease in chronic liver disease and cirrhosis: a nationwide population-based study." *Atherosclerosis* 270 (2018): 154-159.
24. Cláudia, BM Strey, et al. "Impact of diabetes mellitus and insulin on nonalcoholic fatty liver disease in the morbidly obese." *Annals of hepatology* 17.4 (2018): 585-591.
25. Catharina, Arthur Santa, et al. "Metabolic syndrome-related features in controlled and resistant hypertensive subjects." *Arquivos brasileiros de cardiologia* 110.6 (2018): 514-521.
26. Kupčová, Viera, et al. "Overview of the pathogenesis, genetic, and non-invasive clinical, biochemical, and scoring methods in the assessment of NAFLD." *International journal of environmental research and public health* 16.19 (2019): 3570.
27. Lonardo, Amedeo, et al. "Nonalcoholic fatty liver disease: a precursor of the metabolic syndrome." *Digestive and Liver disease* 47.3 (2015): 181-190.
28. Nascimbeni, Fabio, et al. "From NAFLD in clinical practice to answers from guidelines." *Journal of hepatology* 59.4 (2013): 859-871.
29. Hu, Xiao-Yu, et al. "Risk factors and biomarkers of non-alcoholic fatty liver disease: an observational cross-sectional population survey." *BMJ open* 8.4 (2018): e019974.
30. Sheth, Harsh, et al. "The HAALT non-invasive scoring system for NAFLD in obesity." *Obesity surgery* 29.8 (2019): 2562-2570.
31. Yilmaz, Y., and E. Ulukaya. "Toward a biochemical diagnosis of NASH: insights from pathophysiology for distinguishing simple steatosis from steatohepatitis." *Current medicinal chemistry* 18.5 (2011): 725-732.
32. Jennison, Erica, et al. "Diagnosis and management of non-alcoholic fatty liver disease." *Postgraduate medical journal* 95.1124 (2019): 314-322.
33. Singh, Siddharth, et al. "Fibrosis progression in nonalcoholic fatty liver vs nonalcoholic steatohepatitis: a systematic review and meta-analysis of paired-biopsy studies." *Clinical gastroenterology and hepatology* 13.4 (2015): 643-654.
34. Hazlehurst, Jonathan M., et al. "Non-alcoholic fatty liver disease and diabetes." *Metabolism* 65.8 (2016): 1096-1108.

35. Buzzetti, Elena, Massimo Pinzani, and Emmanuel A. Tsochatzis. "The multiple-hit pathogenesis of non-alcoholic fatty liver disease (NAFLD)." *Metabolism* 65.8 (2016): 1038-1048.
36. Ballestri, Stefano, et al. "The independent predictors of non-alcoholic steatohepatitis and its individual histological features. Insulin resistance, serum uric acid, metabolic syndrome, alanine aminotransferase and serum total cholesterol are a clue to pathogenesis and candidate targets for treatment." *Hepatology Research* 46.11 (2016): 1074-1087.
37. Borrelli, Antonella, et al. "Role of gut microbiota and oxidative stress in the progression of non-alcoholic fatty liver disease to hepatocarcinoma: Current and innovative therapeutic approaches." *Redox biology* 15 (2018): 467-479.
38. Gonzalez-Jaramillo, Valentina, et al. "Epigenetics and inflammatory markers: a systematic review of the current evidence." *International journal of inflammation* 2019 (2019).
39. Huang, Paul L. "A comprehensive definition for metabolic syndrome." *Disease models & mechanisms* 2.5-6 (2009): 231-237.
40. Kim, Soon Sun, et al. "Nonalcoholic fatty liver disease as a sentinel marker for the development of diabetes mellitus in non-obese subjects." *Digestive and Liver Disease* 50.4 (2018): 370-377.
41. HaGani, Neta, et al. "The Relationships between Adolescents' Obesity and the Built Environment: Are They City Dependent?." *International journal of environmental research and public health* 16.9 (2019): 1579.
42. Choudhury, Jayanta, and Arun J. Sanyal. "Insulin resistance and the pathogenesis of nonalcoholic fatty liver disease." *Clinics in liver disease* 8.3 (2004): 575-594.
43. Bazick, Jessica, et al. "Clinical model for NASH and advanced fibrosis in adult patients with diabetes and NAFLD: guidelines for referral in NAFLD." *Diabetes care* 38.7 (2015): 1347-1355.
44. Portillo-Sanchez, Paola, et al. "High prevalence of nonalcoholic fatty liver disease in patients with type 2 diabetes mellitus and normal plasma aminotransferase levels." *The Journal of Clinical Endocrinology & Metabolism* 100.6 (2015): 2231-2238.
45. Kwok, Raymond, et al. "Screening diabetic patients for non-alcoholic fatty liver disease with controlled attenuation parameter and liver stiffness measurements: a prospective cohort study." *Gut* 65.8 (2016): 1359-1368.

46. Lonardo, Amedeo, and Paola Loria. "Apolipoprotein synthesis in nonalcoholic steatohepatitis." *Hepatology* 36.2 (2002): 514-515.
47. Greco, Dario, et al. "Gene expression in human NAFLD." *American Journal of Physiology-Gastrointestinal and Liver Physiology* 294.5 (2008): G1281-G1287.
48. Fabbrini, Elisa, et al. "Intrahepatic fat, not visceral fat, is linked with metabolic complications of obesity." *Proceedings of the National Academy of Sciences* 106.36 (2009): 15430-15435.
49. Kupčová, Viera, et al. "Overview of the pathogenesis, genetic, and non-invasive clinical, biochemical, and scoring methods in the assessment of NAFLD." *International journal of environmental research and public health* 16.19 (2019): 3570.
50. Jiang, Weiwei, et al. "Dysbiosis gut microbiota associated with inflammation and impaired mucosal immune function in intestine of humans with non-alcoholic fatty liver disease." *Scientific reports* 5.1 (2015): 1-7.
51. Kirpich, Irina A., Luis S. Marsano, and Craig J. McClain. "Gut–liver axis, nutrition, and non-alcoholic fatty liver disease." *Clinical biochemistry* 48.13-14 (2015): 923-930.
52. Romeo, Stefano, et al. "Genetic variation in PNPLA3 confers susceptibility to nonalcoholic fatty liver disease." *Nature genetics* 40.12 (2008): 1461-1465.
53. Anderson, Nora, and Jürgen Borlak. "Molecular mechanisms and therapeutic targets in steatosis and steatohepatitis." *Pharmacological reviews* 60.3 (2008): 311-357.
54. Joshi-Barve, Swati, et al. "Palmitic acid induces production of proinflammatory cytokine interleukin-8 from hepatocytes." *Hepatology* 46.3 (2007): 823-830.
55. Persico, Marcello, et al. "Suppressor of cytokine signaling 3 (SOCS3) expression and hepatitis C virus–related chronic hepatitis: insulin resistance and response to antiviral therapy." *Hepatology* 46.4 (2007): 1009-1015.
56. Torisu, Takehiro, et al. "The dual function of hepatic SOCS3 in insulin resistance in vivo." *Genes to Cells* 12.2 (2007): 143-154.
57. Browning, Jeffrey D., and Jay D. Horton. "Molecular mediators of hepatic steatosis and liver injury." *The Journal of clinical investigation* 114.2 (2004): 147-152.
58. Bell, Ming, et al. "Consequences of lipid droplet coat protein downregulation in liver cells: abnormal lipid droplet metabolism and induction of insulin resistance." *Diabetes* 57.8 (2008): 2037-2045.

59. Sanyal, Arun J., et al. "Nonalcoholic steatohepatitis: association of insulin resistance and mitochondrial abnormalities." *Gastroenterology* 120.5 (2001): 1183-1192.
60. Tiniakos, Dina G., Miriam B. Vos, and Elizabeth M. Brunt. "Nonalcoholic fatty liver disease: pathology and pathogenesis." *Annual Review of Pathology: Mechanisms of Disease* 5 (2010): 145-171.
61. Lonardo, Amedeo, et al. "Perspectives on cellular dysfunction in nonalcoholic steatohepatitis: a case of 'multiorganelle failure'? Proceedings of a virtual workshop on nonalcoholic steatohepatitis." *Expert review of gastroenterology & hepatology* 5.2 (2011): 135-139.
62. Macaluso, Fabio Salvatore, Marcello Maida, and Salvatore Petta. "Genetic background in nonalcoholic fatty liver disease: A comprehensive review." *World Journal of Gastroenterology: WJG* 21.39 (2015): 11088.
63. Sanal, Madhusudana Girija. "Biomarkers in nonalcoholic fatty liver disease-the emperor has no clothes?." *World Journal of Gastroenterology: WJG* 21.11 (2015): 3223.
64. Romeo, Stefano, et al. "Genetic variation in PNPLA3 confers susceptibility to nonalcoholic fatty liver disease." *Nature genetics* 40.12 (2008): 1461-1465.
65. Bruschi, Francesca Virginia, et al. "The PNPLA3 I148M variant modulates the fibrogenic phenotype of human hepatic stellate cells." *Hepatology* 65.6 (2017): 1875-1890.
66. Sookoian, Silvia, and Carlos J. Pirola. "Meta-analysis of the influence of I148M variant of patatin-like phospholipase domain containing 3 gene (PNPLA3) on the susceptibility and histological severity of nonalcoholic fatty liver disease." *Hepatology* 53.6 (2011): 1883-1894.
67. Kozlitina, Julia, et al. "Exome-wide association study identifies a TM6SF2 variant that confers susceptibility to nonalcoholic fatty liver disease." *Nature genetics* 46.4 (2014): 352-356.
68. Speliotes, Elizabeth K., et al. "Genome-wide association analysis identifies variants associated with nonalcoholic fatty liver disease that have distinct effects on metabolic traits." *PLoS Genet* 7.3 (2011): e1001324.
69. <https://medlineplus.gov/genetics>
70. Mashek, Douglas G. "Hepatic fatty acid trafficking: multiple forks in the road." *Advances in nutrition* 4.6 (2013): 697-710.

71. Koo, Seung-Hoi. "Nonalcoholic fatty liver disease: molecular mechanisms for the hepatic steatosis." *Clinical and molecular hepatology* 19.3 (2013): 210.
72. Falcon, Alaric, et al. "FATP2 is a hepatic fatty acid transporter and peroxisomal very long-chain acyl-CoA synthetase." *American Journal of Physiology-Endocrinology and Metabolism* 299.3 (2010): E384-E393.
73. Doege, Holger, et al. "Targeted deletion of FATP5 reveals multiple functions in liver metabolism: alterations in hepatic lipid homeostasis." *Gastroenterology* 130.4 (2006): 1245-1258.
74. Doege, Holger, et al. "Silencing of hepatic fatty acid transporter protein 5 in vivo reverses diet-induced non-alcoholic fatty liver disease and improves hyperglycemia." *Journal of Biological Chemistry* 283.32 (2008): 22186-22192.
75. Zhu, Lixin, et al. "Lipid in the livers of adolescents with nonalcoholic steatohepatitis: combined effects of pathways on steatosis." *Metabolism* 60.7 (2011): 1001-1011.
76. Westerbacka, Jukka, et al. "Genes involved in fatty acid partitioning and binding, lipolysis, monocyte/macrophage recruitment, and inflammation are overexpressed in the human fatty liver of insulin-resistant subjects." *Diabetes* 56.11 (2007): 2759-2765.
77. Ipsen, David Højland, Jens Lykkesfeldt, and Pernille Tveden-Nyborg. "Molecular mechanisms of hepatic lipid accumulation in non-alcoholic fatty liver disease." *Cellular and molecular life sciences* 75.18 (2018): 3313-3327.
78. Toth, Peter P. "Triglyceride-rich lipoproteins as a causal factor for cardiovascular disease." *Vascular health and risk management* 12 (2016): 171.
79. <https://www.ncbi.nlm.nih.gov/books/NBK351/>
80. Miller, Michael, et al. "Triglycerides and cardiovascular disease: a scientific statement from the American Heart Association." *Circulation* 123.20 (2011): 2292-2333.
81. Do, Ron, et al. "Common variants associated with plasma triglycerides and risk for coronary artery disease." *Nature genetics* 45.11 (2013): 1345-1352.
82. Brahm, Amanda, and Robert A. Hegele. "Hypertriglyceridemia." *Nutrients* 5.3 (2013): 981-1001.
83. Varbo, Anette, et al. "Remnant cholesterol as a causal risk factor for ischemic heart disease." *Journal of the American College of Cardiology* 61.4 (2013): 427-436.

84. Thomsen, Mette, et al. "Low nonfasting triglycerides and reduced all-cause mortality: a mendelian randomization study." *Clinical chemistry* 60.5 (2014): 737-746.
85. Younossi, Zobair M., et al. "Global epidemiology of nonalcoholic fatty liver disease—meta-analytic assessment of prevalence, incidence, and outcomes." *Hepatology* 64.1 (2016): 73-84.
86. Højland Ipsen, David, Pernille Tveden-Nyborg, and Jens Lykkesfeldt. "Normal weight dyslipidemia: is it all about the liver?." *Obesity* 24.3 (2016): 556-567.
87. Wattacheril, Julia, and Arun J. Sanyal. "Lean NAFLD: an underrecognized outlier." *Current hepatology reports* 15.2 (2016): 134-139.
88. Nguyen, P. H. U. O. N. G. T. R. A. N. G., et al. "Liver lipid metabolism." *Journal of animal physiology and animal nutrition* 92.3 (2008): 272-283.
89. Bechmann, Lars P., et al. "The interaction of hepatic lipid and glucose metabolism in liver diseases." *Journal of hepatology* 56.4 (2012): 952-964.
90. Mashek, Douglas G. "Hepatic fatty acid trafficking: multiple forks in the road." *Advances in nutrition* 4.6 (2013): 697-710.
91. Koo, Seung-Hoi. "Nonalcoholic fatty liver disease: molecular mechanisms for the hepatic steatosis." *Clinical and molecular hepatology* 19.3 (2013): 210.
92. Silverstein, Roy L., and Maria Febbraio. "CD36, a scavenger receptor involved in immunity, metabolism, angiogenesis, and behavior." *Science signaling* 2.72 (2009): re3-re3.
93. Qiu, Yan, et al. "Upregulation of caveolin-1 and SR-B1 in mice with non-alcoholic fatty liver disease." *Hepatobiliary & Pancreatic Diseases International* 12.6 (2013): 630-636.
94. Sanders, Francis WB, and Julian L. Griffin. "De novo lipogenesis in the liver in health and disease: more than just a shunting yard for glucose." *Biological Reviews* 91.2 (2016): 452-468.
95. Eberlé, Delphine, et al. "SREBP transcription factors: master regulators of lipid homeostasis." *Biochimie* 86.11 (2004): 839-848.
96. Yamashita, Hiromi, et al. "A glucose-responsive transcription factor that regulates carbohydrate metabolism in the liver." *Proceedings of the national academy of sciences* 98.16 (2001): 9116-9121.

97. Reddy, Janardan K., and M. Sambasiva Rao. "Lipid metabolism and liver inflammation. II. Fatty liver disease and fatty acid oxidation." *American Journal of Physiology-Gastrointestinal and Liver Physiology* 290.5 (2006): G852-G858.
98. Rao, M. Sambasiva, and Janardan K. Reddy. "Peroxisomal β -oxidation and steatohepatitis." *Seminars in liver disease*. Vol. 21. No. 01. Copyright© 2001 by Thieme Medical Publishers, Inc., 333 Seventh Avenue, New York, NY 10001, USA. Tel.:+ 1 (212) 584-4662, 2001.
99. Young, S. G. "Recent progress in understanding apolipoprotein B." *Circulation* 82.5 (1990): 1574-1594.
100. Crooke, Rosanne M., et al. "An apolipoprotein B antisense oligonucleotide lowers LDL cholesterol in hyperlipidemic mice without causing hepatic steatosis." *Journal of lipid research* 46.5 (2005): 872-884.
101. Lee, Richard G., et al. "Comparison of the pharmacological profiles of murine antisense oligonucleotides targeting apolipoprotein B and microsomal triglyceride transfer protein." *Journal of lipid research* 54.3 (2013): 602-614.
102. Wierzbicki, Anthony S., Tim Hardman, and William T. Prince. "Future challenges for microsomal transport protein inhibitors." *Current vascular pharmacology* 7.3 (2009): 277-286.
103. Conlon, Donna M., et al. "Inhibition of apolipoprotein B synthesis stimulates endoplasmic reticulum autophagy that prevents steatosis." *The Journal of clinical investigation* 126.10 (2016): 3852-3867.
104. Feingold, Kenneth R., and Carl Grunfeld. "Lipids: a key player in the battle between the host and microorganisms¹." *Journal of lipid research* 53.12 (2012): 2487-2489.
105. <https://www.ncbi.nlm.nih.gov/books/NBK305896/>
106. Feingold, Kenneth R., et al. "Introduction to Lipids and Lipoproteins--Endotext." (2000).
107. Rogers, Lindsay D., and Christopher M. Overall. "Proteolytic post-translational modification of proteins: proteomic tools and methodology." *Molecular & Cellular Proteomics* 12.12 (2013): 3532-3542.

108. Uy, Rosa, and Finn Wold. "Posttranslational covalent modification of proteins." *Science* 198.4320 (1977): 890-896.
109. Walsh, Gary, and Roy Jefferis. "Post-translational modifications in the context of therapeutic proteins." *Nature biotechnology* 24.10 (2006): 1241-1252.
110. Seidah, Nabil G., and Annik Prat. "The biology and therapeutic targeting of the proprotein convertases." *Nature reviews Drug discovery* 11.5 (2012): 367-383.
111. Seidah, Nabil G., Abdel Majid Khatib, and Annik Prat. "The proprotein convertases and their implication in sterol and/or lipid metabolism." *Biological chemistry* 387.7 (2006): 871-877.
112. Puente, X.S., Sanchez, L.M., Overall, C.M. & Lopez-Otin, C. Human and mouse proteases: a comparative genomic approach. *Nat Rev Genet* 4, 544-558 (2003).
113. Seidah, Nabil G., et al. "The secretory proprotein convertase neural apoptosis-regulated convertase 1 (NARC-1): liver regeneration and neuronal differentiation." *Proceedings of the National Academy of Sciences* 100.3 (2003): 928-933.
114. Seidah, N. G., and J. Guillemot. "Molecular Neuroendocrinology: From Genome to Physiology." (2016): 171-194.
115. Seidah, Nabil G., and Annik Prat. "The biology and therapeutic targeting of the proprotein convertases." *Nature reviews Drug discovery* 11.5 (2012): 367-383.
116. Zhou, An, et al. "Regulatory roles of the P domain of the subtilisin-like prohormone convertases." *Journal of Biological Chemistry* 273.18 (1998): 11107-11114.
117. Furuta, Machi, et al. "Incomplete processing of proinsulin to insulin accompanied by elevation of Des-31, 32 proinsulin intermediates in islets of mice lacking active PC2." *Journal of Biological Chemistry* 273.6 (1998): 3431-3437.
118. Rouillé, Yves, et al. "Role of the prohormone convertase PC3 in the processing of proglucagon to glucagon-like peptide 1." *Journal of Biological Chemistry* 272.52 (1997): 32810-32816.
119. Benjannet, S., et al. "Structure-function studies on the biosynthesis and bioactivity of the precursor convertase PC2 and the formation of the PC2/7B2 complex." *FEBS letters* 362.2 (1995): 151-155.

120. Benjannet, S., et al. "PC1 and PC2 are proprotein convertases capable of cleaving proopiomelanocortin at distinct pairs of basic residues." *Proceedings of the National Academy of Sciences* 88.9 (1991): 3564-3568.
121. Thomas, Gary. "Furin at the cutting edge: from protein traffic to embryogenesis and disease." *Nature reviews Molecular cell biology* 3.10 (2002): 753-766.
122. Lusson, J., et al. "cDNA structure of the mouse and rat subtilisin/kexin-like PC5: a candidate proprotein convertase expressed in endocrine and nonendocrine cells." *Proceedings of the National Academy of Sciences* 90.14 (1993): 6691-6695.
123. Essalmani, Rachid, et al. "Deletion of the gene encoding proprotein convertase 5/6 causes early embryonic lethality in the mouse." *Molecular and Cellular Biology* 26.1 (2006): 354-361.
124. Nakagawa, Tsutomu, et al. "Identification and functional expression of a new member of the mammalian Kex2-like processing endoprotease family: its striking structural similarity to PACE4." *The Journal of Biochemistry* 113.2 (1993): 132-135.
125. Nakagawa, Tsutomu, Kazuo Murakami, and Kazuhisa Nakayama. "Identification of an isoform with an extremely large Cys-rich region of PC6, a Kex2-like processing endoprotease." *FEBS letters* 327.2 (1993): 165-171.
126. Constam, Daniel B., and Elizabeth J. Robertson. "SPC4/PACE4 regulates a TGF β signaling network during axis formation." *Genes & development* 14.9 (2000): 1146-1155.
127. Guillemot, Johann, et al. "Implication of the proprotein convertases in iron homeostasis: proprotein convertase 7 sheds human transferrin receptor 1 and furin activates hepcidin." *Hepatology* 57.6 (2013): 2514-2524.
128. Seidah, Nabil G. "Proprotein convertase subtilisin kexin 9 (PCSK9) inhibitors in the treatment of hypercholesterolemia and other pathologies." *Current pharmaceutical design* 19.17 (2013): 3161-3172.
129. Poirier, Steve, et al. "The proprotein convertase PCSK9 induces the degradation of low density lipoprotein receptor (LDLR) and its closest family members VLDLR and ApoER2." *Journal of Biological Chemistry* 283.4 (2008): 2363-2372.
130. Liu, Dajiang J., et al. "Exome-wide association study of plasma lipids in > 300,000 individuals." *Nature genetics* 49.12 (2017): 1758-1766.

131. Manning, Alisa K., et al. "A genome-wide approach accounting for body mass index identifies genetic variants influencing fasting glycemic traits and insulin resistance." *Nature genetics* 44.6 (2012): 659-669.
132. Scott, Robert A., et al. "An expanded genome-wide association study of type 2 diabetes in Europeans." *Diabetes* 66.11 (2017): 2888-2902.
133. McInnes, Gregory, et al. "Global Biobank Engine: enabling genotype-phenotype browsing for biobank summary statistics." *Bioinformatics* 35.14 (2019): 2495-2497.
134. Malik, Rainer, et al. "Multiancestry genome-wide association study of 520,000 subjects identifies 32 loci associated with stroke and stroke subtypes." *Nature genetics* 50.4 (2018): 524-537.
135. Peloso, Gina M., et al. "Association of low-frequency and rare coding-sequence variants with blood lipids and coronary heart disease in 56,000 whites and blacks." *The American Journal of Human Genetics* 94.2 (2014): 223-232.
136. (Sachan V. et al., unpublished)
137. Kozlitina, Julia, et al. "Exome-wide association study identifies a TM6SF2 variant that confers susceptibility to nonalcoholic fatty liver disease." *Nature genetics* 46.4 (2014): 352-356.
138. Holmen, Oddgeir L., et al. "Systematic evaluation of coding variation identifies a candidate causal variant in TM6SF2 influencing total cholesterol and myocardial infarction risk." *Nature genetics* 46.4 (2014): 345-351.
139. Kozlitina, Julia, et al. "Exome-wide association study identifies a TM6SF2 variant that confers susceptibility to nonalcoholic fatty liver disease." *Nature genetics* 46.4 (2014): 352-356.
140. Kozlitina, Julia, et al. "Exome-wide association study identifies a TM6SF2 variant that confers susceptibility to nonalcoholic fatty liver disease." *Nature genetics* 46.4 (2014): 352-356.
141. Holmen, O. L., H. Zhang, and Y. Fan. "Hovelson DH, Schmidt EM, Zhou W, Guo Y, et al. Systematic evaluation of coding variation identifies a candidate causal variant in TM6SF2 influencing total cholesterol and myocardial infarction risk." *Nat Genet* 46.4 (2014): 345-351.

142. Sookoian, Silvia, et al. "Genetic variation in transmembrane 6 superfamily member 2 and the risk of nonalcoholic fatty liver disease and histological disease severity." *Hepatology* 61.2 (2015): 515-525.
143. Dongiovanni, Paola, et al. "Transmembrane 6 superfamily member 2 gene variant disentangles nonalcoholic steatohepatitis from cardiovascular disease." *Hepatology* 61.2 (2015): 506-514.
144. Falletti, Edmondo, et al. "PNPLA3 rs738409 and TM6SF2 rs58542926 variants increase the risk of hepatocellular carcinoma in alcoholic cirrhosis." *Digestive and Liver Disease* 48.1 (2016): 69-75.
145. Goffredo, Martina, et al. "Role of TM6SF2 rs58542926 in the pathogenesis of nonalcoholic pediatric fatty liver disease: A multiethnic study." *Hepatology* 63.1 (2016): 117-125.
146. Smagris, Eriks, et al. "Inactivation of Tm6sf2, a gene defective in fatty liver disease, impairs lipidation but not secretion of very low density lipoproteins." *Journal of Biological Chemistry* 291.20 (2016): 10659-10676.
147. Ehrhardt, Nicole, et al. "Hepatic Tm6sf2 overexpression affects cellular ApoB-trafficking, plasma lipid levels, hepatic steatosis and atherosclerosis." *Human molecular genetics* 26.14 (2017): 2719-2731.
148. Li, Bo-Tao, et al. "Disruption of the ERLIN–TM6SF2–APOB complex destabilizes APOB and contributes to non-alcoholic fatty liver disease." *PLoS genetics* 16.8 (2020): e1008955.

Supplemental Images:

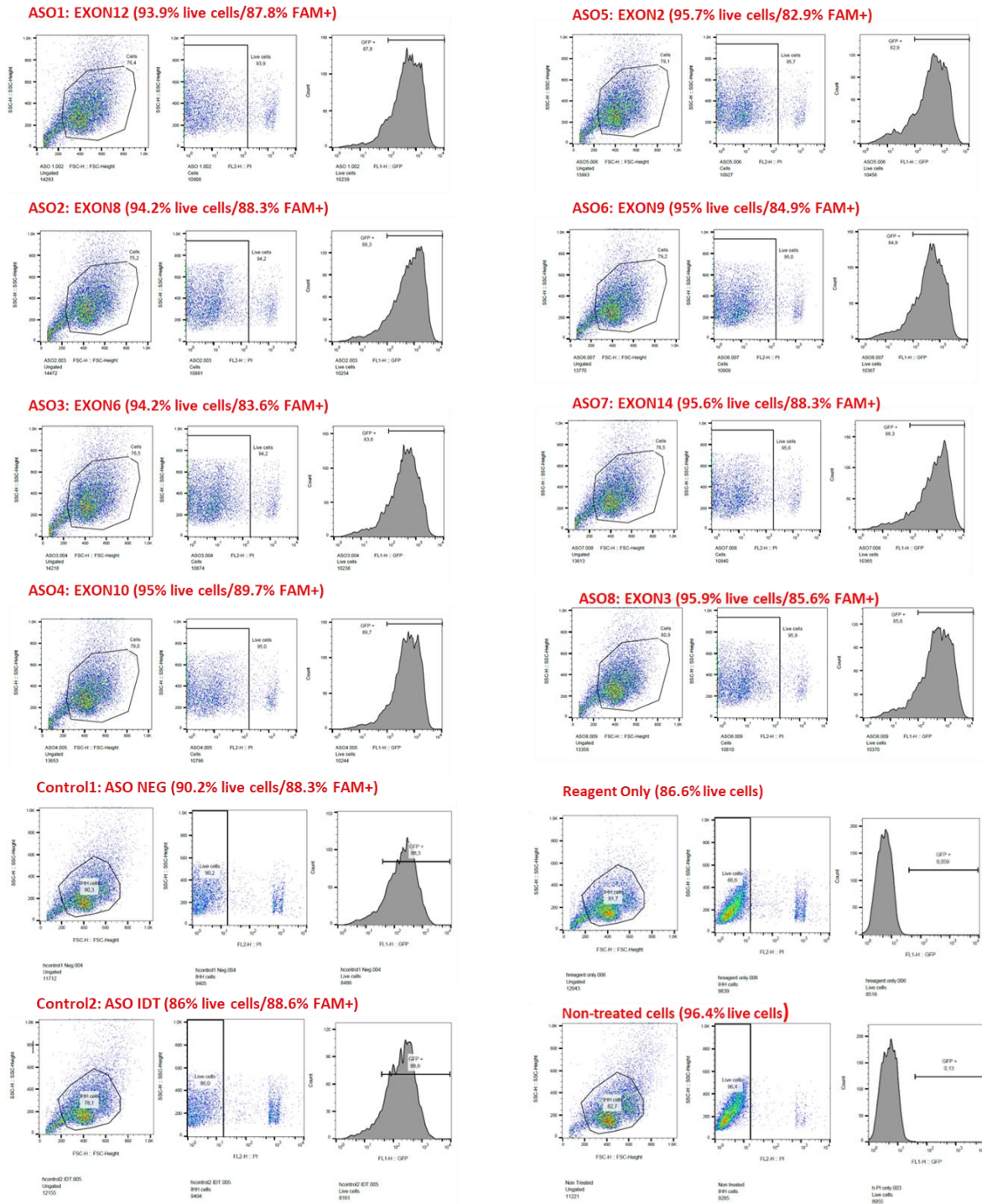
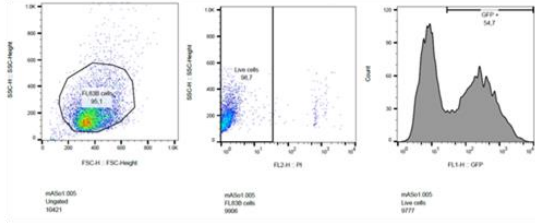
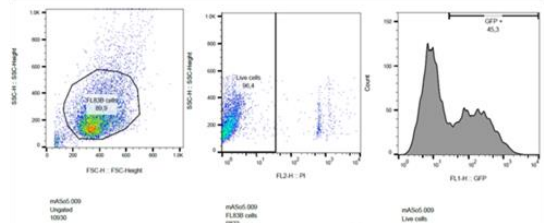


Figure 24. FACS results for the transfection efficiency of ASOs (IHH, Dharmafect/25 nM ASOs/24hrs)

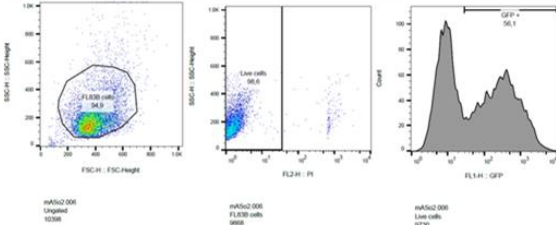
ASO1: EXON17 (98.7% live cells/54.7% FAM+)



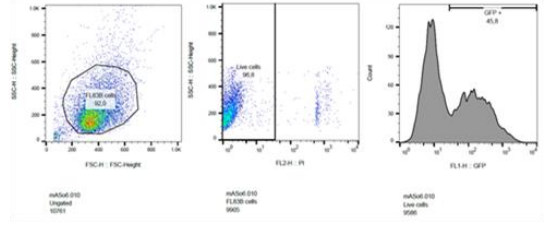
ASO5: EXON12 (96.4% live cells/45.3% FAM+)



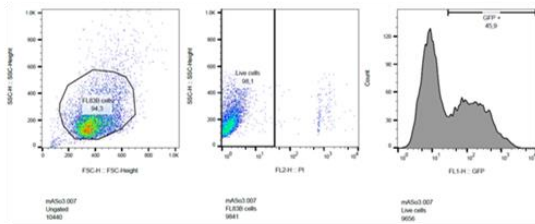
ASO2: EXON6 (98.6% live cells/56.1% FAM+)



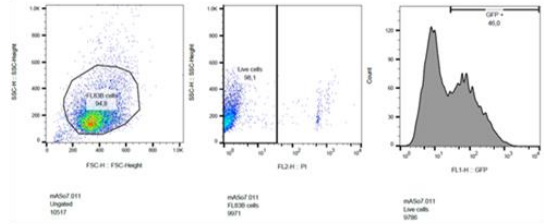
ASO6: EXON2 (96.8% live cells/45.8% FAM+)



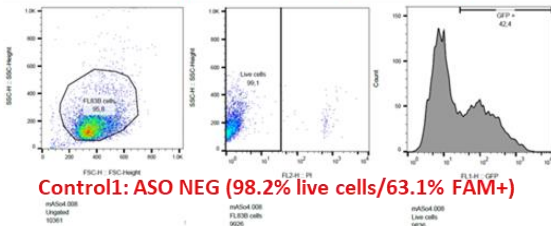
ASO3: EXON14 (98.1% live cells/45.9% FAM+)



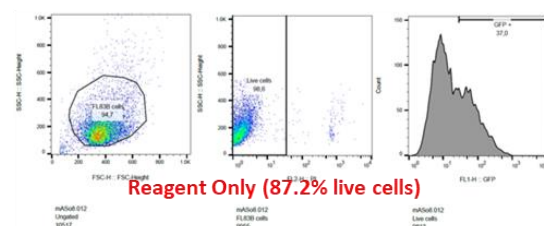
ASO7: EXON4 (98.1% live cells/46% FAM+)



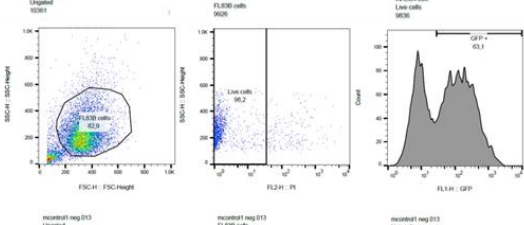
ASO4: EXON8 (99.1% live cells/42.4% FAM+)



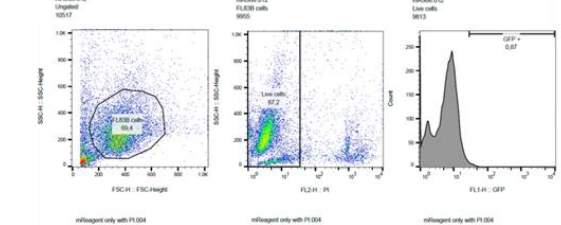
ASO8: EXON5 (98.6% live cells/37% FAM+)



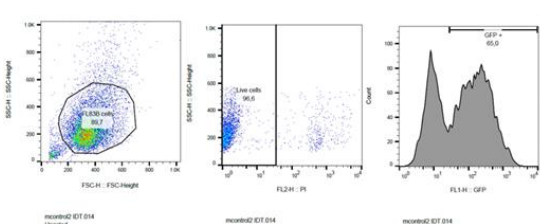
Control1: ASO NEG (98.2% live cells/63.1% FAM+)



Reagent Only (87.2% live cells)



Control2: ASO IDT (96.6% live cells/65% FAM+)



Non-treated cells (99.6% live cells)

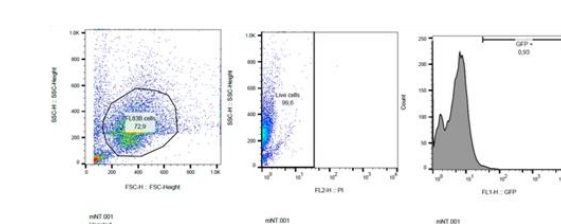


Figure 25. FACS results for the transfection efficiency of ASOs (FL83B, Dharmafect/25 nM ASOs/24hrs)